A review on thermophysical properties and thermal stability of sugar alcohols as phase change materials

A Review on Thermophysical Properties and Thermal Stability of Sugar Alcohols as Phase Change Materials

Sebastiano Tomassetti[a,*], Alessia Aquilanti[a,b], Pio Francesco Muciaccia[a], Gianluca Coccia[a], Christoph Mankel[b], Eduardus A.B. Koenders[b], Giovanni Di Nicola[a]

[a] *Marche Polytechnic University, Department of Industrial Engineering and Mathematical Sciences, Via Brecce Bianche 12, 60131, Ancona (Italy)*
[b] *Technical University of Darmstadt, Institute of Construction and Building Materials, Franziska-Braun-Str. 3, 64287, Darmstadt (Germany)*

Abstract

The increasing use of renewable energy sources has highlighted the importance of energy storages, and in particular of latent heat thermal energy storages (LHTESs). Among the phase change materials (PCMs) that can be used in such systems, sugar alcohols (SAs) are considered potential substances that may lead to interesting applications in the LHTES sector. In this work, a detailed literature review analysis of six SAs (xylitol, sorbitol, erythritol, mannitol, inositol, dulcitol), their thermophysical properties, their thermal stability and their main LHTES applications is presented for the first time. The thermophysical properties under discussion include melting and crystallization temperatures, latent heats of melting and crystallization, specific heat, thermal conductivity, density and dynamic viscosity. Thermal stability was evaluated by taking into account studies of thermal endurance, degradation temperature and cycling stability. Differential scanning calorimetry (DSC), T-history, Fourier transform infrared spectroscopy (FTIR) and thermogravimetric analysis (TGA) were considered as measurement techniques. Applications include the use of SAs in solar collectors

*Corresponding author. Tel: +39 0712204277, fax: +39 0712204770
Email addresses: s.tomassetti@pm.univpm.it (Sebastiano Tomassetti), a.aquilanti@pm.univpm.it (Alessia Aquilanti), p.f.muciaccia@pm.univpm.it (Pio Francesco Muciaccia), g.coccia@univpm.it (Gianluca Coccia), mankel@wib.tu-darmstadt.de (Christoph Mankel), koenders@wib.tu-darmstadt.de (Eduardus A.B. Koenders), g.dinicola@univpm.it (Giovanni Di Nicola)

and cookers, heat exchangers, porous materials, absorption cooling systems, mobilized thermal energy storages (M-TESs). New measurements of phase transition properties and degradation temperature for the studied SAs were also carried out by the authors of the present study. A good agreement between the proposed data and the literature values was found. The analysis reveals that some SAs may be considered suitable for low-to-medium temperature LHTES applications, provided that their drawbacks are adequately evaluated and addressed. To this purpose, the study also highlights the most critical aspects that should be considered when developing both fundamental research and engineering applications related to SAs.

Keywords: sugar alcohol; latent heat thermal energy storage; nucleation triggering; thermal stability; differential scanning calorimetry; T-history

---

1. Introduction

From several years, numerous thermal energy storage (TES) systems have been studied to improve the use of renewable and sustainable energy sources and the industrial waste heat recovery [1, 2, 3]. Among the three main types of TES systems (i.e., sensible, latent, and thermochemical), the latent heat thermal energy storage (LHTES) systems relying on phase change materials (PCMs) are among the most attractive techniques for storing thermal energy [4, 5, 6, 7]. LHTES systems exploit PCMs' phase transitions, usually from solid to liquid and vice versa, to store or retrieve heat energy in the form of latent heat, allowing a higher storage density than that of the sensible TES systems.

The performance of a great number of solid-liquid PCMs having melting temperatures and physical properties to develop LHTES systems to be used in many applications has been investigated in recent years [8, 9, 10, 11]. Among the main applications, there are solar energy [5, 1], building sector [12, 13, 14, 15], cold storage [8, 11], industrial sector [14, 16, 17].

In the selection process of PCMs and in the design of LHTES systems, a reliable and accurate knowledge of their thermophysical properties is fundamental.

This is also essential to develop reliable mathematical models to analyze their thermal performance in specific LHTES applications [18, 19]. For this purpose, experimental data of different thermophysical properties for numerous materials have been measured using specific measurement methods [20, 21]. The values of melting (T_m) and crystallization temperature (T_c), latent heat of melting (ΔH_m) and crystallization (ΔH_c), as well as specific heat (c_p), can be determined through thermal analysis techniques as a function of temperature or time. The differential scanning calorimetry (DSC) and the T-history method are two of the most widespread and well-known techniques for the measurements of these properties. The DSC is a widely used and standardized non-isothermal method allowing to accurately measure T_m, T_c, ΔH_m, ΔH_c, and c_p by subjecting the samples to controlled heating/cooling rates [22, 21, 23]. However, this analysis technique has various limitations [22, 21], among which: a small amount of material is measured (masses of about few milligrams); the thermal response is influenced by the sample mass and the used heating/cooling rate; lack of repeatability may occur for heterogeneous samples; in composite materials, the main component can interfere in the measurement signal. In addition, the DSC is an expensive device and the analysis of a material can be time-consuming as the DSC allows to analyze only one sample at a time [21, 24].

The T-history method is a simple isothermal method that allows to simultaneously measure T_m, T_c, ΔH_m, ΔH_c, and c_p of samples of a few grams by subjecting them to constant charge/discharge temperatures [21, 25, 26]. Since the samples tested with the T-history method are larger than those measured with the DSC and are exposed to constant charge/discharge temperatures, the results of the T-history method are considered to be closer to the real bulk properties of the studied materials [27, 28, 26, 29]. Moreover, the T-history method is less expensive and less time-consuming than the DSC, enabling simultaneous measurements of more samples. However, one of the main drawbacks of this analysis technique is the lack of standardization, which does not allow an accurate comparison between the values provided by different apparatus. Also, different mathematical models were used to derive the values of the properties

from the measurements [27, 24].

In addition, to assess if a PCM is suitable for practical LHTES applications, an accurate knowledge of its thermal stability under application conditions is fundamental [30, 31]. It is necessary to distinguish between: thermal endurance, degradation temperature, and long-term thermal stability or cycling stability. The thermal endurance tests allow to evaluate the variations of the physical and chemical characteristics and the thermal performance of PCMs as function of time by keeping them at different constant working temperatures higher than their melting points [32]. The chemical stability of PCMs is generally evaluated by the Fourier transform infrared spectroscopy (FTIR) [30]. The degradation temperature analysis determines the maximum temperature of a PCM below which the material does not show thermal decomposition. It is usually carried out by means of the thermogravimetric analysis (TGA) technique [33]. The long-term stability of PCMs is analyzed by performing several consecutive thermal cycles of heating and cooling with the aim to evaluate if the materials show deterioration of thermal performance and/or degradation [30, 34]. Since no standard procedures for long-term stability analysis have been developed, different techniques taking into account various application conditions (e.g., temperature interval, heating and cooling rates, contact to atmosphere, contact to container, container material, sample size) have been employed [20, 30, 34].

As evident in Table 1, which provides the advantages and disadvantages of some of the main classes of PCMs, it is unlikely to find materials that completely fulfill all the characteristics required by ideal PCMs [5, 35, 36, 37, 38]. In this regard, several solid-liquid PCMs have drawbacks that could hinder their use for different applications [7, 39]: the phenomenon of supercooling, also named subcooling (i.e, the possibility for the PCM to release its latent heat at a temperature lower than melting point during solidification), low thermal conductivity, low long-term thermal stability, high flammability, corrosiveness, high variations of pressure and volume in phase transitions, leakage of molten PCMs into the surrounding of the LHTES system, and so on. In particular, some materials show high and stable supercooling which results in difficult nucleation trigger-

Table 1: Advantages and disadvantages of organic, inorganic, end eutectic PCMs.

	Organic materials			**Inorganic materials**		**Eutectics**
	Sugar alcohols	*Paraffins*	*Fatty acids*	*Salt hydrates*	*Metallic with low* T_{m}	
Advantages	•High latent heat of melting •No phase segregation •Compatibility with conventional materials of construction •Non-flammability •Safe and no-reactive •Non-toxic •Low environmental impact •Available in quantity •Recyclable	•Good latent heat of melting •Absence of supercooling •No phase segregation •Congruent melting •Chemical stability •Compatible with all metal containers •Available in quantity •Safe •Non-corrosive •Recyclable	•High latent heat of melting •Sharp phase transformation •Absence of supercooling •Reproducible melting and freezing behavior •Recyclable	•High latent heat of melting per unit of volume •High thermal conductivity •High density •Sharp melting point •Compatible with plastics containers •Non-flammability •Low environmental impact •Available in quantity •Inexpensive	•High latent heat of melting per unit of volume •High thermal conductivity •Low vapor pressure	•High volumetric thermal storage density •Good thermal conductivity •Sharp melting temperature •No phase segregation and congruent phase change
Disadvantages	•Low thermal conductivity •High degree of supercooling •Lack of thermal stability •Prone to degradation	•Lack of a well-defined sharp melting point •Low thermal conductivity •Low density •Incompatible with plastic container •High volume change •Volatile •Moderately flammable •Expensive	•Low thermal conductivity •Instable at high temperature •Highly inflammable •Low flash point •Toxic •Mild corrosive •Expensive	•Supercooling •Phase segregation •Chemically instable when heated •High vapor pressure •Incongruent melting •Corrosion on metal containers •No thermal stability •Slightly toxic •Irritant	•Low latent heat of melting per unit of weight •Low specific heat capacity •Non-flammable •Expensive	•Low latent heat of melting per unit of weight •Some eutectics suffer from supercooling •Expensive •Data of their thermophysical properties are often limited

ing [40]. Consequently, numerous methods to overcome these issues of PCMs and improve their performance have been evaluated and are still under study [41, 42, 43, 44, 45].

As can be noted in Table 1, a promising class of PCMs that can limit some of the aforementioned issues includes sugar alcohols (SAs). Thus, for the first time, this work aims to review the available literature studies presenting experimentally-determined thermophysical properties and thermal tests for six sugar polyalcohols (xylitol, sorbitol, erythritol, mannitol, inositol, dulcitol), i.e. organic materials considered potential solid-liquid PCMs for low-to-medium temperature LHTESs (80–250 °C). This study also provides new measurements of phase transition properties and degradation temperature for the analyzed sugar alcohols. The main purpose of this literature review is to provide a clear overview about the experimentally-determined properties and thermal performances of SAs which have advantages but also different drawbacks for their use as PCMs in LHTES applications. To evaluate their behavior in real applications, the use of SAs as PCMs in LHTES systems has also been reviewed. Therefore, unlike other literature reviews regarding PCMs that analyze the state of the art of PCMs or their use in dedicated applications, this review is specifically oriented to evaluate the characteristics of this promising class of PCMs.

The paper is organized as follows. Section 2 provides an overview of the sugar alcohols studied in the present work. The same section depicts the methodological details used to carry out the experimental measurements of the considered SAs. Section 3 includes a literature survey of the main thermophysical properties available for the SAs. Detailed tables have been provided with experimental data of T_{m}, T_{c}, ΔH_{m}, ΔH_{c}, ρ (density) and μ (dynamic viscosity), while several graphs are available with points and trends for c_{p} and λ (thermal conductivity). Section 4 discusses the thermal stability of SAs, and in particular their thermal endurance, degradation temperatures and cycling stability. Section 5 provides a summary of literature works about LHTES systems using SAs as storage substances. Finally, the conclusions of the study can be found in Section 6.

2. Sugar alcohols and measurement methods

This section presents the sugar alcohols reviewed in this work. In addition, the methods employed to carry out the measurements of the properties presented in the study are described.

2.1. Sugar alcohols

Sugar alcohols (SAs), also known as polyalcohols, polyols, hydrogenated carbohydrates or polyhydric alcohols, are hydrogenated forms of carbohydrates, in which the carboxyl group (either aldehyde or ketone) has been reduced to a primary or secondary hydroxyl group, hence alcohol [46]. They belong to the low molecular weight carbohydrate family, have an OH group attached to all the carbon atoms, and are described by the following general formula: $C_nH_{2n+2}O_n$. SAs are characterized by different chain length (i.e., a different number of carbon atoms) and relative orientation of the OH groups. Usually, they are classified into the following two groups: glycitols or acyclic polyols, having linear chains with three to seven carbon atoms (or more when they are branched), and cyclitols or cyclic polyols, such as inositol and inositol derivatives. They can be either of natural origin or derived with chemical processes from carbohydrates reduction. Many of them are commonly used as sweeteners to replace sugar in the pharmaceutical and food industries to develop products suitable for diabetics and non-cariogenic food [47, 48].

As described in the literature [16, 49], the use of SAs as PCMs was firstly proposed by Hormansdorfer [50]; then, their phase change properties were analyzed by Barone et al. [51] and Talja and Roos [52]. Almost all the SAs having suitable properties to be used as PCMs for low-to-medium temperature LHTES systems are characterized by chains of four to six carbon atoms [53]. As reported in Table 1, in addition to be non-flammable, non-toxic, and usually available in large quantities, these substances have a high latent heat storage capacity with respect to their melting points, higher than that of other organic PCMs such as paraffins. Moreover, as by-products of the food industry, their environmental impact is low [54]. Generally, SAs are indicated as non-corrosive [55, 56];

however, it seems that some of them could be affected by corrosion [57]. The promising SAs for LHTES systems can be further selected on the basis of their prices. In this regard, Shao et al. [53] performed a screening based on their prices at reagent pure grade to select the most cost-effective substances among a list of 17 SAs. They selected six substances: five of which are linear carbon chain SAs, namely xylitol, sorbitol, erythritol, mannitol, and dulcitol (galactitol); the other one is a cyclic carbon chain SA, called inositol. Three of them (i.e., sorbitol, mannitol, and dulcitol) are isomers with 6 carbon atoms. A new analysis of the prices of the SAs reported in Table 2 and obtained from two manufactures (Sigma-Aldrich and Fisher Scientific) confirms the results presented by Shao et al. [53]. Considering also that these six substances and their eutectic mixtures are some of the most investigated SAs to be used as PCMs [55, 56, 58, 53], the properties of the six SAs are reviewed in this work.

It was shown in the literature that, despite their aforementioned promising properties, most of the selected SAs exhibits severe issues that could hinder their use as PCMs (Table 1). A detailed analysis of the drawbacks of the studied SAs based on the data collected from the reviewed works is reported in the following sections.

Moreover, it is important to point out that, to evaluate the possibility of using this class of materials in a wider temperature range, the thermophysical properties and the thermal stability of different eutectic mixtures of SAs have been analyzed in several studies [58, 55, 29, 56, 59]. It was shown that these eutectic mixtures generally have lower latent heats of fusion than those of the individual components, and also a severe supercooling [53]. On the other hand, some of them showed a better thermal endurance and thermal cycling stability with respect to their individual components [60, 61].

A general description about the characteristics and production for each SA analyzed in this work (i.e., xylitol, sorbitol, erythritol, mannitol, inositol, and dulcitol) is reported below. Table 3 shows the health hazard of the studied SAs provided in the National Fire Protection Association (NFPA) 704 [62] diamond standard.

Table 2: Price information of some of the sugar alcohols selected by Shao et al. [53] available for purchase from Sigma-Aldrich and Fisher Scientific.

Sugar alcohol	CAS number	Sources	Purity %	Max. available pack size (g)[a]	Price (EUR/g)[a]
erythritol	149-32-6	Sigma-Aldrich	≥99	100.0	3.04
		Fisher Scientific	99	100.0	1.50
l-threitol	2319-57-5	Sigma-Aldrich	99	1.0	131.00
adonitol	488-81-3	Sigma-Aldrich	≥99	100.0	6.49
		Fisher Scientific	98	500.0	3.38
l-arabitol	7643-75-6	Sigma-Aldrich	pss[b]	1.0	79.00
		Fisher Scientific	99	100.0	4.79
d-arabitol	488-82-4	Sigma-Aldrich	≥99	100.0	13.40
		Fisher Scientific	99	100.0	4.84
xylitol	87-99-0	Sigma-Aldrich	≥99	1000.0	0.36
		Fisher Scientific	99	500.0	0.21
inositol	87-89-8	Sigma-Aldrich	≥99	1000.0	0.38
		Fisher Scientific	99	500.0	0.32
l-iditol	488-45-9	Sigma-Aldrich	≥98	0.1	1050.00
d-mannitol	69-65-8	Sigma-Aldrich	≥98	5000.0	0.10
		Fisher Scientific	≥97	5000.0	0.04
d-sorbitol	50-70-4	Sigma-Aldrich	≥99	5000.0	0.22
		Fisher Scientific	98	2000.0	0.04
d-dulcitol (or galactiol)	608-66-2	Sigma-Aldrich	≥99	100.0	0.84
		Fisher Scientific	≥99	500.0	0.44
allitol	488-44-8	Sigma-Aldrich	99.89	0.025	6834.80

[a] information obtained from the official websites of the sources (accessed November 2021): https://www.sigmaaldrich.com and https://www.fishersci.it

[b] pharmaceutical secondary standard

Table 3: Health hazard of the studied SAs reported in the National Fire Protection Association (NFPA) 704 [62] diamond standard.

Sugar alcohol	Health hazard	Fire hazard	Instability - reactivity
Xylitol	1[a]	1[b]	0[c]
Sorbitol	1[a]	1[b]	0[c]
Erythritol	1[a]	1[b]	0[c]
Mannitol	1[a]	1[b]	0[c]
Inositol	1[a]	0[d]	0[c]
Dulcitol	0[e]	0[d]	0[c]

[a] Significant irritation.

[b] It requires preheating for ignition.

[c] It is normally stable, even under fire exposure conditions, and is not reactive with water.

[d] It will not burn under normal fire conditions.

[e] No health hazard.

2.1.1. Xylitol

Xylitol ($C_5H_{12}O_5$, CAS Number 87-99-0, molar mass of 152.15 g/mol) is a linear carbon chain SA having 5 carbon atoms. This SA is produced industrially by catalytic hydrogenation of the sugar D-xylose which is obtained from xylan-containing materials, e.g. birch, strawberry, raspberry, plum, and wheat [48, 63]. Xylitol can present two crystalline forms [48]: a metastable, hygroscopic monoclinic form having a T_m between 61–61.5 °C, and a stable, orthorhombic form having a T_m between 93–94.5 °C. The measured sample of xylitol considered in the present work was purchased from Sigma-Aldrich and its purity was $\geq$ 99 %.

2.1.2. Sorbitol

D-sorbitol ($C_6H_{14}O_6$, CAS Number 50-70-4, molar mass of 182.17 g/mol), less commonly known as glucitol, is a linear carbon chain SA having 6 carbon atoms. It is produced industrially by catalytic hydrogenation using glucose or sucrose as raw materials [48, 63]. Sorbitol can be naturally found in different fruits and some vegetables. Sorbitol is characterized by polymorphism; the gamma crystalline form with a T_m between 95.3–98 °C is the most stable form

[48, 64]. The measured sample of sorbitol considered in the present work was purchased from Sigma-Aldrich and its purity was $\geq$ 99.5 %.

2.1.3. Erythritol

Meso-erythritol ($C_4H_{10}O_4$, CAS number 149-32-6, molar mass of 122.12 g/mol) is a linear carbon chain SA having 4 carbon atoms. Since the high cost of substrate erythrose needed for its production by direct catalytic hydrogenation, it is produced industrially by a fermentation process led by osmophilic yeasts or some species of lactic acid bacteria [63]. Small quantities of erythritol can be naturally found in some vegetables, fruits, and fermented foods. Erythritol can present two crystalline forms [65]: a stable crystalline form with a T_{m} of about 117 °C and a metastable crystalline form with a T_{m} of about 104 °C. The measured sample of meso-erythritol considered in the present work was purchased from Sigma-Aldrich and its purity was $\geq$ 99%.

2.1.4. Mannitol

D-mannitol ($C_6H_{14}O_6$, CAS number 69-65-8, molar mass of 182.172 g/mol) is a linear carbon chain SA having 6 carbon atoms. Since it can be found naturally in high amounts in different trees, it can be produced through extraction from natural sources. However, this type of production is not considered economically important; therefore, mannitol is mainly produced industrially from the catalytic hydrogenation of glucose/fructose (1:1) mixture [48, 63]. Mannitol is characterized by polymorphism; the beta crystalline form with a T_{m} of about 157 °C is the most stable one [66]. The measured sample of d-mannitol considered in the present work was purchased from Sigma-Aldrich and its purity was $\geq$ 98%.

2.1.5. Inositol

Myo-inositol ($C_6H_{12}O_6$, CAS number 87-89-8, molar mass of 180.16 g/mol) is a cyclic carbon chain SA having 6 carbon atoms. Among the nine different stereoisomers of inositol, myo-inositol is the most abundant [67]. Inositol is usually produced industrially by the acid hydrolysis of phytate, which is extracted

from the bran and seeds of plants [67, 68]. Myo-inositol is an essential growth factor in tissues without comas, plant and animal tissues, fungi and some bacteria. It is contained in cereals with a high bran content (buckwheat), beans, fruit and nuts [67, 68]. Myo-inositol is characterized by polymorphism; the alpha monoclinic anhydrate crystalline form with T_{m} between 225 °C and 238 °C is the stable one [69]. The measured sample of myo-inositol considered in the present work was purchased from Sigma-Aldrich and its purity was $\geq$ 99%.

2.1.6. Dulcitol

D-dulcitol ($C_6H_{14}O_6$, CAS number 608-66-2, molar mass of 182.172 g/mol), also known as galactitol, is a linear carbon chain SA having 6 carbon atoms. D-dulcitol is usually obtained from the process of hydrogenation of galactose, which is a functional component in plants and animals [70, 71, 72]. The measured sample of dulcitol considered in the present work was purchased from Sigma-Aldrich and its purity was $\geq$ 99%.

2.2. Methods

A differential scanning calorimeter (NETZSCH DSC 214 POLYMA) was used to measure T_{m}, T_{c}, ΔH_{m}, and ΔH_{c} of the studied SAs. For each substance, three different samples of approximately 10 mg each were firstly weighed by a WAAGEN-Kissling Sartorius microbalance and subsequently placed into aluminum crucibles with perforated lids. The characterization of each sample was carried out by performing three continuous heating/cooling cycles at a heating/cooling rate of 1 °C/min over specific temperature ranges. In detail, according to the melting temperature of each SA, the instrument was set as follows: (25 to 30) °C – (30 to 120) °C – (120 to 30) °C for xylitol; (25 to 30) °C – (30 to 130) °C – (130 to 30) °C for sorbitol; (25 to 30) °C – (30 to 140) °C – (140 to 30) °C for erythritol; (25 to 100) °C – (100 to 200) °C – (200 to 100) °C for mannitol; (25 to 160) °C – (160 to 250) °C – (250 to 160) °C for inositol; (25 to 100) °C – (100 to 210) °C – (210 to 100) °C for dulcitol.

A thermogravimetric analysis (TGA) was performed to measure the mass

variation of the six selected sugar alcohols as a function of temperature. The analyses were performed using a NETZSCH STA 449 F5 JUPITER system using nitrogen as purge gas in the sample chamber. Aluminum crucibles, one for each selected SAs, were filled with about 34 mg of substance and preheated at 40 °C for 30 minutes. Subsequently, each substance was further heated at a constant heating rate of 20 °C/min. In detail, the instrument was set to reach a temperature of 350 °C for erythritol, 400 °C for mannitol, 450 °C for dulcitol, and 500 °C for xylitol, sorbitol, and inositol.

3. Thermophysical properties

This section presents a comparison and a discussion of the results obtained from a literature survey of some of the main thermophysical properties for the studied SAs (i.e., temperatures and latent heats of the melting and crystallization points, specific heats, thermal conductivity, viscosity, and density). Although it is not claimed that the presented survey is exhaustive, a wide-ranging and in-depth search of the experimentally-determined properties for the analyzed substances available in the open literature was performed. The collected data were selected considering specific selection criteria reported below.

3.1. Melting and crystallization properties

The literature values of melting temperature (T_{m}), crystallization temperature (T_{c}), latent heat of melting (ΔH_{m}), and latent heat of crystallization (ΔH_{c}) for the six SAs are reported in this section, together with the DSC measurements carried out by us. The data for xylitol and erythritol measured by us have been also reported elsewhere [73, 74]. The values collected from the literature were selected by following these criteria.

- The measurements performed using a differential scanning calorimeter (DSC) or a T-history method were collected.
- Among the studies reporting measurements performed using a DSC, only the ones providing experimental data of all the aforementioned properties

were selected. As will be explained below, it was not taken into account for xylitol and sorbitol.

The selected data of T_m, T_c, ΔH_m, and ΔH_c measured with a DSC are reported in Table 4 for xylitol, Table 5 for sorbitol, Table 6 for erythritol, Table 7 for mannitol, Table 8 for inositol, and Table 9 for dulcitol. If not otherwise stated, T_m and T_c correspond to onset temperatures. In addition, these tables show the available measurement uncertainties, heating/cooling rates, and sample purities reported in the selected works.

From the data reported in the tables, the followings considerations can be stated.

- While different DSC measurements of the studied properties for xylitol (Table 4), sorbitol (Table 5), erythritol (Table 6), and mannitol (Table 7) are available in the open literature, a very limited number of works reporting experimental data for inositol (Table 8) and dulcitol (Table 9) have been found.

- As shown by the standard deviations reported in the tables, the collected values of T_m for all the studied sugars are generally consistent with each other, while the discrepancy between the measurements of ΔH_m is slightly higher. This is also evident in Figure 1, which shows the experimental data of ΔH_m vs. T_m for erythritol. In particular, few T_m and ΔH_m measurements differ from their mean values by more than two times their standard deviations. These differences can be due to the purity of the samples or the accuracy of the measurement setup and procedure. Moreover, the experimental data for T_m and ΔH_m are generally almost independent of the heating rate used for the measurements.

- The melting properties of the six SAs evaluated by us in this work are consistent with the selected literature. Their absolute relative deviations respect to the mean values are always less than 2 % for T_m and 6 % for ΔH_m.

Table 4: Measurements of melting temperature (onset) (T_{m}) and latent heat of melting (ΔH_{m}) for **xylitol** carried out with DSC at various heating rates (HR).

T_{m} (°C)	ΔH_{m} (J/g)	HR (°C/min)	Purity %	Reference
92.0	249.0	0.5	i.q.[a]	[75]
92.8	241.2	0.5	99	[76]
93.0 ± 1.0	236.0 ± 4.0	0.5	f.g.[b]	[77]
92.5 ± 0.1	246 ± 2	1	-	[51]
92.7	240.1	1	99	[55]
95.1[c]	251.0	1	99	[56]
92.0 ± 0.5	232.7 ± 9.2	1	≥ 99	this work
93.0	245.0 ± 5.0	2	≥99	[78]
93.1	226.2	5	≥99	[79]
93.4 ± 0.3	237.5 ± 3.5	5	99	[53]
93.3 ± 0.2	231.4 ± 2.5	5	98	[53]
93.0 ± 1.0	241.0 ± 2.0	5	f.g.[b]	[77]
92.7 ± 0.1	232.0 ± 1.0	5	>99	[52]
95.0[c]	248.0	5	-	[80]
93.0	280.0	5	>99	[81]
92.0	243.3	5	99	[82]
95.0	267.0	10	>98	[58]
93.0	259.7	10	99	[83]
93.0 ± 0.5	263.0 ± 13.0	10	>98	[54]
90.0 ± 1.0	237.6 ± 1.3	10	t.g.[d]	[84]
91.1	286.6	10	-	[85]
94.4[e]	221.4 ± 2.2	10	>99	[86]
92.7	273.0	10	>98	[87]
95.7[e]	246.0 ± 1.0	-	>99	[88]
93.0 ± 1.2[f]	**247.3 ± 16.3[f]**	**-**	**-**	**-**

[a] industrial quality [b] food grade

[c] unspecified type of temperature [d] technical grade

[e] peak temperature [f] mean value ± standard deviation

Table 5: Measurements of melting temperature (onset) (T_m) and latent heat of melting (ΔH_m) for **sorbitol** carried out with DSC at various heating rates (HR).

T_m (°C)	ΔH_m (J/g)	HR (°C/min)	Purity %	Reference
93.2	153.0	1	99.5	[55]
100.0	185.0	1	98	[56]
93.4 ± 0.3	166.0 ± 2.0	1	-	[51]
95.6 ± 0.3	167.3 ± 6.2	1	≥99.5	this work
95.3 ± 0.5	172.2 ± 4.3	2–5	-	[89]
96.8	217.0	3.5	-	[90]
95.1	132.5	5	≥98	[79]
97.4 ± 0.2	164.0 ± 3.2	5	98	[53]
99.4 ± 0.2	184.4 ± 2.6	5	98	[53]
95.0 ± 1.2	165.0 ± 1.0	5	>97	[52]
97.0	110.0	5	>99	[81]
101.1 ± 0.1[a]	173 ± 5	10	>97	[91]
99.2[b]	168.3 ± 1.7	10	>99	[92]
98.0 ± 0.3	174.0 ± 2.0	10	98.9	[64]
98.8	196.8	10	-	[93]
94.2	135.3	-	-	[94]
96.8 ± 2.3[c]	**166.5 ± 24.7[c]**	**-**	**-**	**-**

[a] unspecified type of temperature [b] peak temperature
[c] mean value ± standard deviation

- As also evident in Figure 2, the temperature range from around 90 °C to over 220 °C is covered by the T_m of the studied six SAs. This proves that they can be considered potential PCMs for low-to-medium temperature LHTES. Moreover, Figure 2 shows that all the studied SAs have mean values of ΔH_m higher that 200 J/g, with the exception of sorbitol. In this regard, it is important to note that, with respect to other PCMs with similar melting point temperatures [35, 7], sorbitol has relatively lower values of ΔH_m (mean value of about 170 J/g) that could hinder its use as PCM. On the other hand, erythritol and dulcitol have the highest mean values of ΔH_m (about 335 J/g for erythritol and about 330 J/g for

Table 6: Measurements of melting temperature (onset) (T_m), latent heat of melting (ΔH_m), crystallization temperature (onset) (T_c), and latent heat of crystallization (ΔH_c) for **erythritol** carried out with DSC at various heating/cooling rates (HR/CR).

T_m (°C)	ΔH_m (J/g)	T_c (°C)	ΔH_c (J/g)	HR/CR (°C/min)	Purity %	Reference
118.8 ± 0.1	325.4 ± 0.6	31.1 ± 0.7	200.5 ± 5.5	0.5	99	[53]
119.0 ± 1.0	329.0 ± 14.0	25.0 ± 28.0	204.0 ± 26.0	0.5[a]	f.g.[b]	[77]
119.0 ± 1.0	329.0 ± 14.0	52.0 ± 30.0	204.0 ± 25.0	0.5[c]	f.g.[b]	[77]
118.3 ± 0.7	327.3 ± 1.3	28.4 ± 1.5	208.5 ± 6.6	1	99	[53]
118.7 ± 0.1	333.1 ± 6.3	56.5 ± 17.7	250.4 ± 19.7	1	≥99	this work
118.1	340.6	38.8	252.3	2	-	[95]
118.8[d]	374.3	55.3[d]	194.1	3	-	[96]
127.5	311.0	53.1	308.2	5	-	[97]
118.9 ± 0.1	332.3 ± 0.8	22.4 ± 5.8	186.3 ± 5.7	5	99	[53]
118.8 ± 0.1	333.7 ± 1.2	16.9 ± 1.8	171.3 ± 5.6	5	99	[53]
116.0 ± 1.0	319.0 ± 20.0	22.0 ± 31.0	101.0 ± 65.0	5[a]	f.g.[b]	[77]
116.0 ± 1.0	319.0 ± 20.0	24.0 ± 20.0	203.0 ± 20.0	5[c]	f.g.[b]	[77]
119.5	328.0	33.5	224.2	5	99	[98]
119.7 ± 0.3	337.8 ± 2.6	18.7 ± 1.1	191.8 ± 6.5	10	99	[53]
118.7	357.3	19.8	141.8	10	-	[99]
118.6	349.9	33.9	224.2	10	c.g.[e]	[100]
118.9	342.2	38.5[f]	213.9	10	99	[101]
118.7	345.3	15.6	127.4	10	a.g.[g]	[102]
119.2 ± 0.1	334.4 ± 3.6	46.5 ± 1.1	224.8 ± 2.3	10	99	[103]
117.2	308.8	20.4	246.6	10	>95	[104]
118.4	310.6	33.0	213.1	10	99	[105]
118.4[d]	379.6	36.2[d]	256.0	10	≥99	[106]
119.0	349.9	33.5	224.2	-	-	[107]
118.9 ± 2.0[h]	**335.5 ± 17.8[h]**	**32.8 ± 12.5[h]**	**207.5 ± 43.5[h]**	**-**	**-**	**-**

[a] in smooth crucible [b] food grade [c] in rough crucible [d] unspecified type of temperature
[e] commercial grade [f] peak temperature [g] analytical grade [h] mean value ± standard deviation

Table 7: Measurements of melting temperature (onset) (T_m), latent heat of melting (ΔH_m), crystallization temperature (onset) (T_c), and latent heat of crystallization (ΔH_c) for **mannitol** carried out with DSC at various heating/cooling rates (HR/CR).

T_m (°C)	ΔH_m (J/g)	T_c (°C)	ΔH_c (J/g)	HR/CR (°C/min)	Purity %	Reference
166.2 ± 0.2	278.6 ± 0.9	118.5 ± 0.1	243.0 ± 0.6	0.5	98	[53]
151.0	234.4	114.1	224.6	1	-	[108]
166.3 ± 0.2	278.7 ± 0.1	119.1 ± 0.1	242.8 ± 0.7	1	98	[53]
165.7	334.5	122.9	234.8	1	≥98	[109]
165.6 ± 0.1	284.3 ± 3.9	120.0 ± 0.2	238.6 ± 6.9	1	≥98	this work
166.1 ± 0.0	281.1 ± 1.3	111.1 ± 1.7	238.3 ± 5.9	5	98	[53]
166.0 ± 0.1	277.4 ± 1.1	114.1 ± 0.6	227.9 ± 0.9	5	99	[53]
166.6 ± 0.1	299.5 ± 0.4	110.9 ± 1.0	234.5 ± 0.7	10	98	[53]
166.4	281.9	120.2	219.5	10	99	[110]
165.3	282.0	123.0	241.3	10	98	[111]
166.2	288.1	115.0	228.0	10	-	[112]
165.0	295.2	109.4	213.0	10	98	[113]
168.8[a]	284.9	107.7[a]	214.4	10	99	[114]
170.2	293.1	118.0	238.2	-	99.5	[115]
165.4 ± 4.2[b]	**285.3 ± 19.9[b]**	**116.0 ± 4.8[b]**	**231.4± 9.9[b]**	**-**	**-**	**-**

[a] peak temperature [b] mean value ± standard deviation

Table 8: Measurements of melting temperature (onset) (T_{m}), latent heat of melting (ΔH_{m}), crystallization temperature (onset) (T_{c}), and latent heat of crystallization (ΔH_{c}) for **inositol** carried out with DSC at various heating/cooling rates (HR/CR).

T_{m} (°C)	ΔH_{m} (J/g)	T_{c} (°C)	ΔH_{c} (J/g)	HR/CR (°C/min)	Purity %	Reference
224.0 ± 0.2	257.1 ± 0.4	186.3 ± 1.7	196.5 ± 0.6	0.5	99	[53]
216.3	185.3	182.3	206.6	1	-	[108]
224.2 ± 0.1	257.6 ± 0.4	185.5 ± 1.9	198.6 ± 0.5	1	99	[53]
224.0 ± 0.2	249.6 ± 8.6	184.4 ± 0.6	191.4 ± 4.6	1	≥99	this work
224.3 ± 0.2	256.3 ± 1.5	180.9 ± 0.2	196.9 ± 1.8	5	99	[53]
224.5 ± 0.2	261.8 ± 0.1	181.4 ± 0.5	198.6 ± 0.2	5	99	[53]
225.5[a]	351.6	185.7[a]	325.8	6	99	[116]
224.8 ± 0.4	256.9 ± 1.0	178.1 ± 0.4	190.4 ± 1.3	10	99	[53]
227.9[a]	260.7	183.8[a]	190.9	10	≥99	[117]
224.9[b]	260.9	191.4[b]	198.0	10	98	[118]
224.0 ± 2.8[c]	**259.8 ± 37.6[c]**	**184.0 ± 3.5[c]**	**209.4 ± 39.1[c]**	**-**	**-**	**-**

[a] peak temperature [b] unspecified type of temperature [c] mean value ± standard deviation

Table 9: Measurements of melting temperature (onset) (T_{m}), latent heat of melting (ΔH_{m}), crystallization temperature (onset) (T_{c}), and latent heat of crystallization (ΔH_{c}) for **dulcitol** carried out with DSC at various heating/cooling rates (HR/CR).

T_{m} (°C)	ΔH_{m} (J/g)	T_{c} (°C)	ΔH_{c} (J/g)	HR/CR (°C/min)	Purity %	Reference
186.4 ± 0.1	322.6 ± 0.7	120.5 ± 1.3	239.5 ± 6.1	0.5	99	[53]
180.1	257.2	102.1	245.7	1	-	[108]
186.0 ± 0.1	323.2 ± 2.1	120.2 ± 1.1	216.8 ± 3.5	1	99	[53]
187.2 ± 0.1	330.0 ± 0.5	120.1 ± 0.8	235.8 ± 2.1	1	≥99	this work
185.9 ± 0.2	334.1 ± 0.6	116.9 ± 2.4	232.4 ± 5.1	5	99	[53]
187.3 ± 0.1	350.8 ± 2.1	116.9 ± 1.3	232.4 ± 0.9	5	98	[53]
187.4	401.8	115.8	285.2	10	≥99	[70]
187.8 ± 0.8	333.5 ± 0.8	113.9 ± 0.9	254.9 ± 0.6	10	99	[53]
186.0 ± 2.3[a]	**331.7 ± 37.1[a]**	**115.8 ± 5.6[a]**	**242.8 ± 19.1[a]**	**-**	**-**	**-**

[a] mean value ± standard deviation

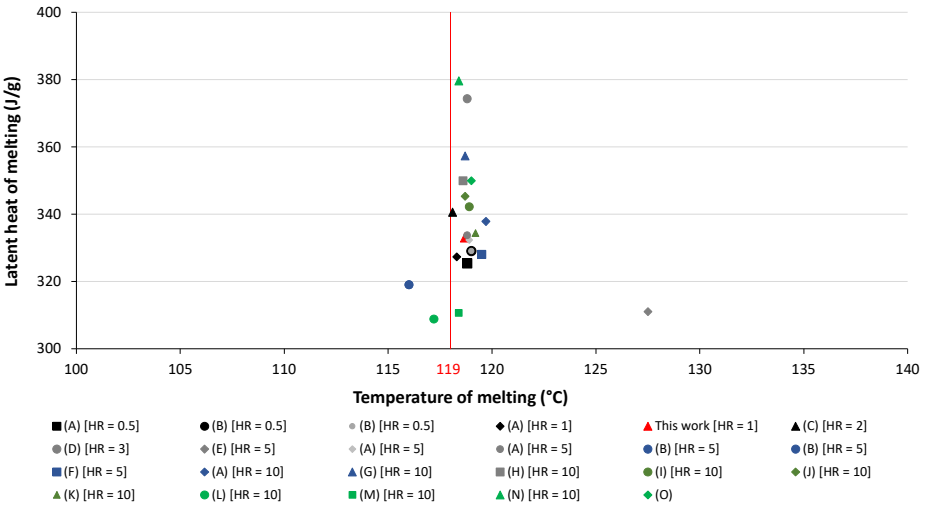

Figure 1: Temperatures of melting vs. latent heats of melting for erythritol of Table 6: (A) [53]; (B) [77]; (C) [95]; (D) [96]; (E) [97]; (F) [98]; (G)[99]; (H) [100]; (I) [101]; (J) [102]; (K) [103]; (L) [104]; (M) [105]; (N) [106]; (O) [107]. The red vertical line indicates the melting temperature and delimits the solid phase (left) from the liquid phase (right). HR is in °C/min.

dulcitol).

- The values of T_c and ΔH_c for xylitol and sorbitol are not reported in Table 4 and Table 5, respectively, because no liquid-solid transition (exothermic peak) was recorded during the cooling phase of the DSC measurements presented in different works [84, 75, 88, 53], even at low temperatures. The same behavior was also found for the samples of xylitol and sorbitol measured by us. In particular, no endothermic peaks were recorded by repeating the DSC measurements in the following heating phase on the same samples, given that no liquid-solid phase transitions occurred during the cooling period of the previous cycle. As explained by different authors [53, 79, 55], these two SAs have a very stable supercooling due to high resistance to crystallization, remaining supercooled liquids until amorphous metastable solid states appear at low temperatures. It was shown that the resistance to crystallization of xylitol is linked to its high degree of cooperation in molecular motion and slow molecular mobility

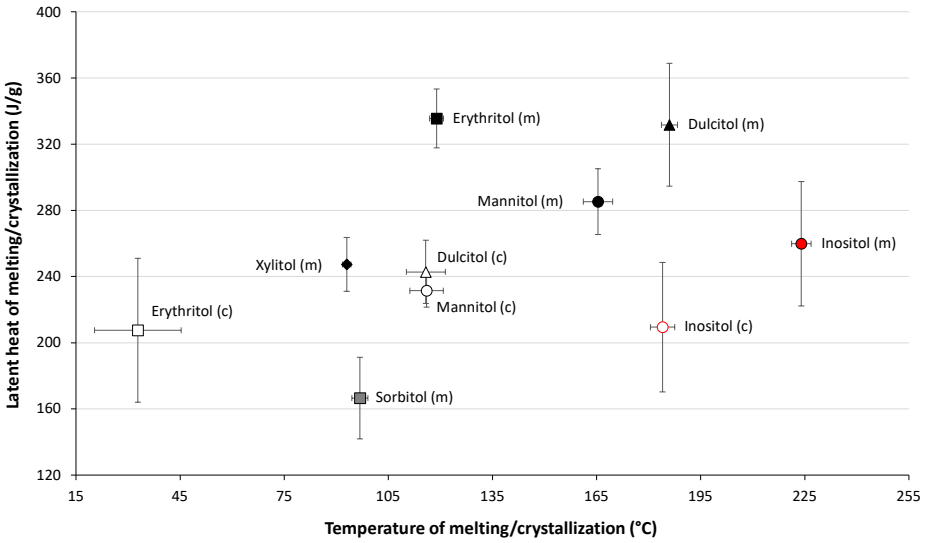

Figure 2: Average melting and crystallization properties of the studied SAs taken from Tables 4 to 9. The bars in the figure indicate the standard deviations of the properties. The letters (m) and (c) indicate the melting and crystallization points, respectively.

[88]. Therefore, the difficulties in crystallization of xylitol and sorbitol should be appropriately taken into account to assess their possible use as PCMs for different LHTES applications. In general, this behavior is considered a significant drawback that could hinder their use as PCMs for short-term LHTESs [119]. But their resistance to crystallization can be regarded as an advantage for the development of seasonal or long-term LHTESs as long as the crystallization can be triggered when the stored heat is needed [56, 54]. However, different experimental and theoretical works [75, 54, 80, 120, 76, 121] showed that the very difficult nucleation triggering and slow growth rate of crystallization of xyilitol could prevent its direct use also in seasonal LHTES applications. In fact, these issues result in a complicated energy discharge triggering and a low discharge power, respectively. For this reason, among the studied active nucleation triggering techniques that allow to release the stored heat on demand [40], methods suitable for these two SAs should be used to ap-

propriately allow energy discharge at the temperatures required for the specific applications. In this regard, different literature works analyzed specific methods to activate the nucleation and crystallization processes of xylitol [122, 120, 76, 73, 121] and to enhance its crystallization rate [75].

- The reported values of T_c and ΔH_c for erythritol (Table 6), mannitol (Table 7), inositol (Table 8), and dulcitol (Table 9) demonstrate that these four SAs have high or low supercooling degree (i.e., the difference between the melting and crystallization temperatures). In fact, as also evident in Figure 2, the mean values for the crystallization point of these SAs are lower than that measured for the melting point. In particular, Figure 2 shows that erythritol has a higher supercooling degree and a higher difference between ΔH_m and ΔH_c than that of the other three SAs. In addition, as shown in Figure 3 for erythritol, the collected experimental data for the crystallization point are more scattered than those measured for the melting point (Figure 1). Although supercooling is still not fully understood [123], it is influenced by numerous causes such as the sample volume, the presence of impurities, the properties of the container, and the cooling conditions [124, 27, 77]. This phenomenon could hinder the use of these SAs as PCMs for different applications. Therefore, specific methods to reduce the supercooling degree of SAs should be considered for their proper use in the LHTES systems. Different passive nucleation triggering techniques that can allow to reduce the supercooling of PCMs, such as the addition of different nucleating agents or their micro-encapsulation, have been widely studied in the literature [40, 43, 44]. In particular, various literature works analyzed the effects of the following techniques to mitigate the supercooling of erythritol: ultrasonic irradiation [125, 123], stirring [125], agitation by bubbling [125, 126], nucleating agents [100, 99, 103], micro-encapsulation [100, 103], and electric current [127]. Finally, it should be stressed that, to accurately model the thermal performance of the studied SAs in specific LHTES applications, it is essential to consider

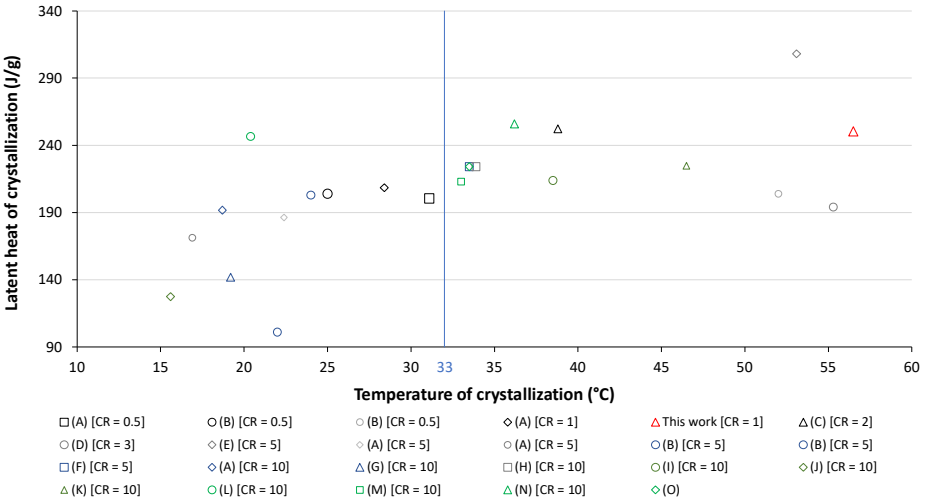

Figure 3: Temperatures of crystallization vs latent heats of crystallization for erythritol of Table 6: (A) [53]; (B) [77]; (C) [95]; (D) [96]; (E) [97]; (F) [98]; (G)[99]; (H) [100]; (I) [101]; (J) [102]; (K) [103]; (L) [104]; (M) [105]; (N) [106]; (O) [107]. The blue vertical line indicates the melting temperature and delimits the solid phase (left) from the liquid phase (right). CR is in °C/min.

simulation approaches addressing their supercooling [128].

As concerns the measurements based on the T-history method, a very limited number of works presenting experimental data for the studied SAs have been found in the literature. In particular, Gunasekara et al. [129] measured T_m and ΔH_m of xylitol and erythritol by using the T-history method. The results demonstrated that erythritol had two different melting temperatures (one at 117–122 °C with an average ΔH_m of 284 kJ/kg and the other at 105–111 °C with an average ΔH_m of 255 kJ/kg) at different cycles and had supercooling. The T_m and ΔH_m of xylitol were found to be 88–96 °C and 159 kJ/kg, respectively. However, no crystallization or melting for xylitol were observed after the first cycle and the sample showed a probable glass-transition. In a more recent study [130], the same authors presented the following values of T_m and ΔH_m measured with the T-history method: 112.6–128.0 °C and 229 kJ/kg for erythritol; 90.6–97.7 °C and 164 kJ/kg for xylitol. Huang et al. [131] obtained a T_m of 162.3 °C

and a ΔH_{m} of 288.4 kJ/kg for mannitol from experimental tests based on the T-history method. The phenomenon of supercooling was also evident in these tests. The following values of T_{m} for five SAs were measured by Shao et al. [29] using the T-history method: 91.4 °C for xylitol, 117.3 °C for erythritol, 161.4 °C for mannitol, 223.6 °C for inositol, and 183.2 °C for dulcitol. These last experimental tests based on the T-history method confirmed that erytritol, mannitol, inositol, and dulcitol suffer supercooling. Instead, the tests for xylitol also showed lack of crystallization during the cooling of the melted sample; the authors explained that xylitol could remain in the state of supercooled liquid until its vitrification occurred at a temperature equal to −22 °C. In addition, they found that the T_{m} of xylitol measured by the T-history method was slightly lower than that obtained with the DSC. This difference was due to the different techniques used to determine the melting temperature. Finally, it can be noted that: the few values of T_{m} and ΔH_{m} measured by means of the T-history method are usually in agreement with the measurements performed with the DSC method; the T-history method also showed the crystallization issues found for the DSC measurements.

3.2. Specific heat

The values of specific heat (c_{p}) for the studied SAs collected from the literature are reported in this section. Figure 4, Figure 5, Figure 6, Figure 7, Figure 8, and Figure 9 show the selected data (both regressed and experimental) of c_{p} for xylitol, sorbitol, erythritol, mannitol, inositol, and dulcitol, respectively, as a function of temperature. In particular, these figures present the behaviors of c_{p} both in the liquid and solid phases at temperatures of interest for the engineering applications (from about 20 °C up to temperatures somewhat higher than their melting points). Almost all the reported c_{p} data were determined from DSC measurements.

From these figures, it can be pointed out that various studies presenting c_{p} data for the analyzed SAs in the studied temperature ranges are available in the literature. The only exception is dulcitol; in fact, three sources presenting

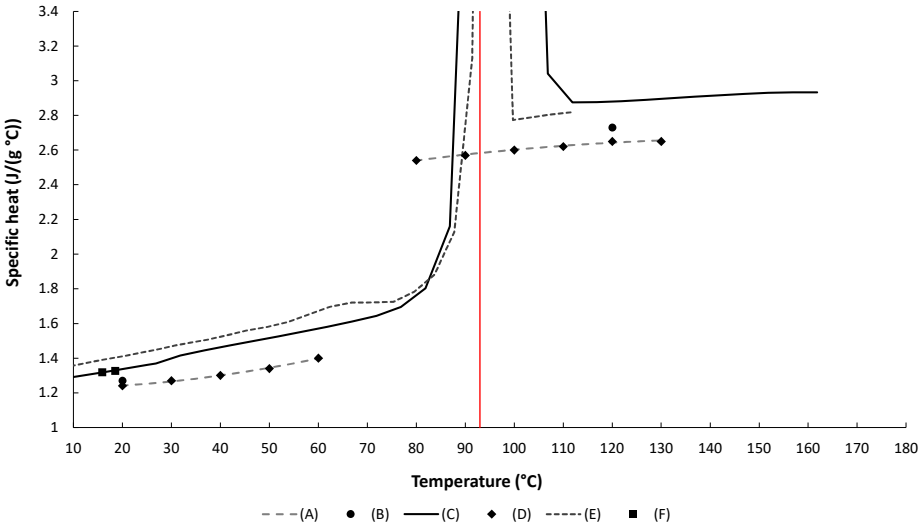

Figure 4: Specific heat values of **xylitol** collected from literature as a function of temperature: (A) [58]; (B) [84]; (C) [83]; (D) [54]; (E) [86]; (F) [132]. The red vertical line indicates the melting temperature and delimits the solid phase (left) from the liquid phase (right).

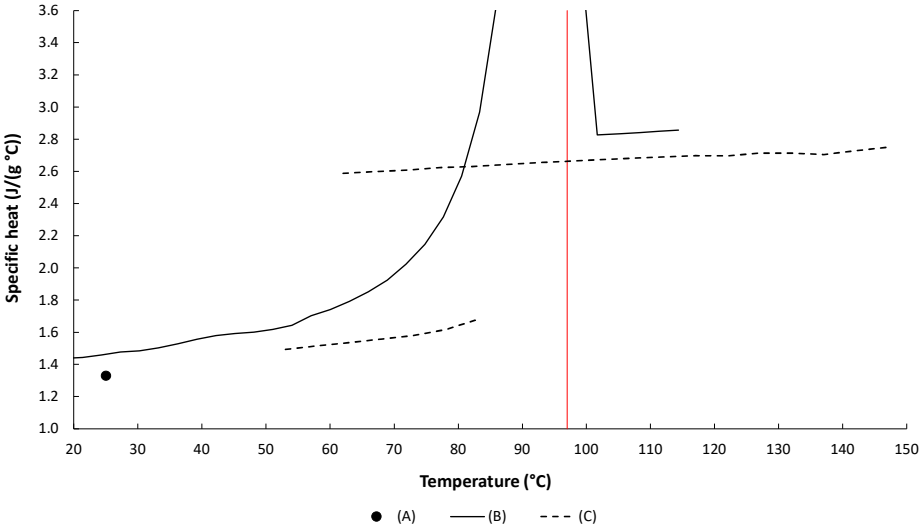

Figure 5: Specific heat values of **sorbitol** collected from literature as a function of temperature: (A) [133]; (B) [92]; (C) [91]. The red vertical line indicates the melting temperature and delimits the solid phase (left) from the liquid phase (right).

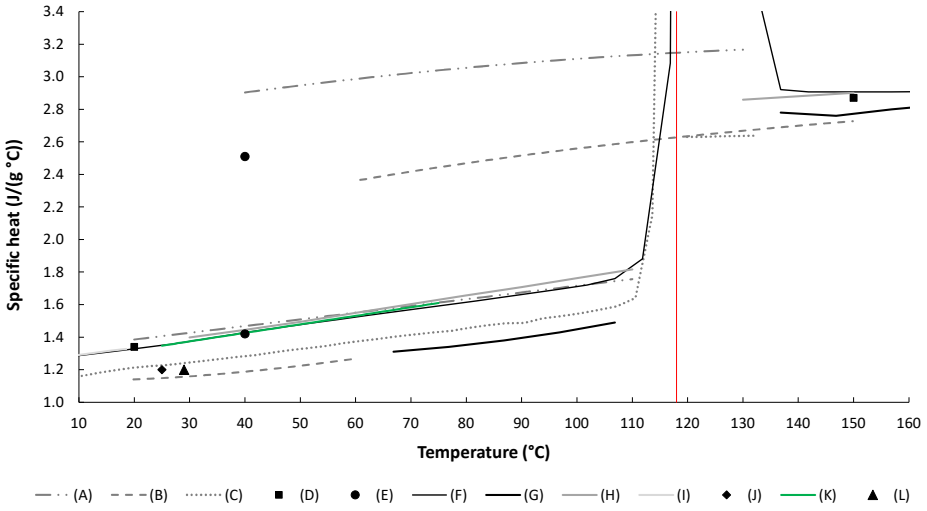

Figure 6: Specific heat values of **erythritol** collected from literature as a function of temperature: (A) [134]; (B) [58]; (C) [135]; (D) [84]; (E) [77]; (F) [83]; (G) [136]; (H) [137]; (I) [132]; (J) [138]; (K) [139]; (L) [140]. The red vertical line indicates the melting temperature and delimits the solid phase (left) from the liquid phase (right).

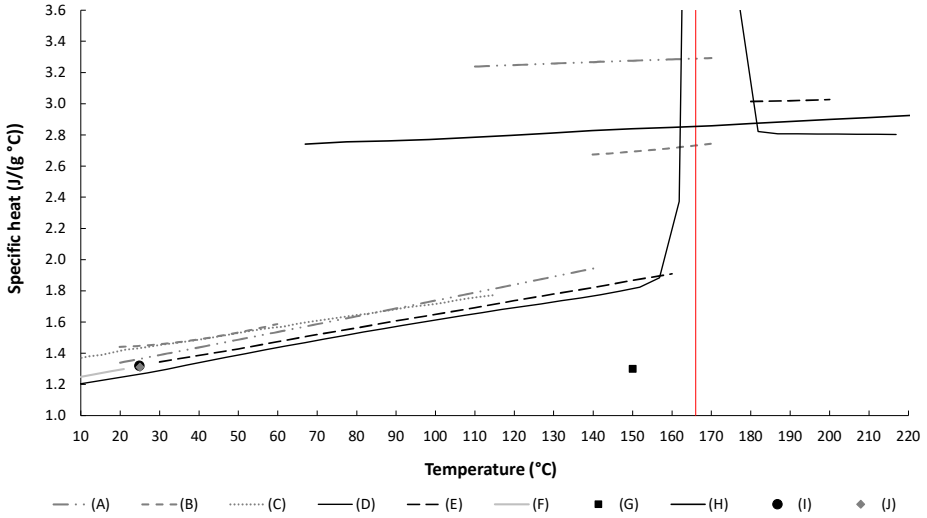

Figure 7: Specific heat values of **mannitol** collected from literature as a function of temperature: (A) [134]; (B) [58]; (C) [141]; (D) [83]; (E) [137]; (F) [132]; (G) [142]; (H) [91]; (I) [143]; (J) [133]. The red vertical line indicates the melting temperature and delimits the solid phase (left) from the liquid phase (right).

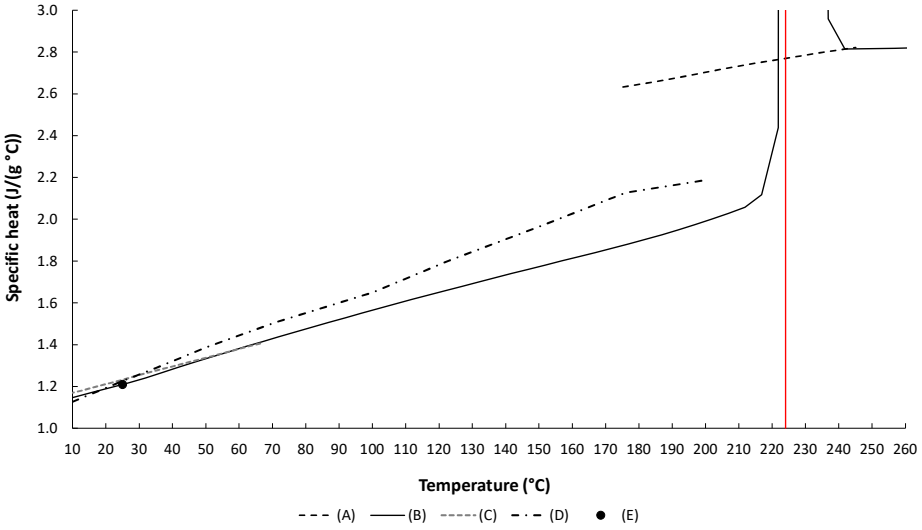

Figure 8: Specific heat values of **inositol** collected from literature as a function of temperature: (A) [91]; (B) [83]; (C) [144]; (D) [145]; (E) [133]. The red vertical line indicates the melting temperature and delimits the solid phase (left) from the liquid phase (right).

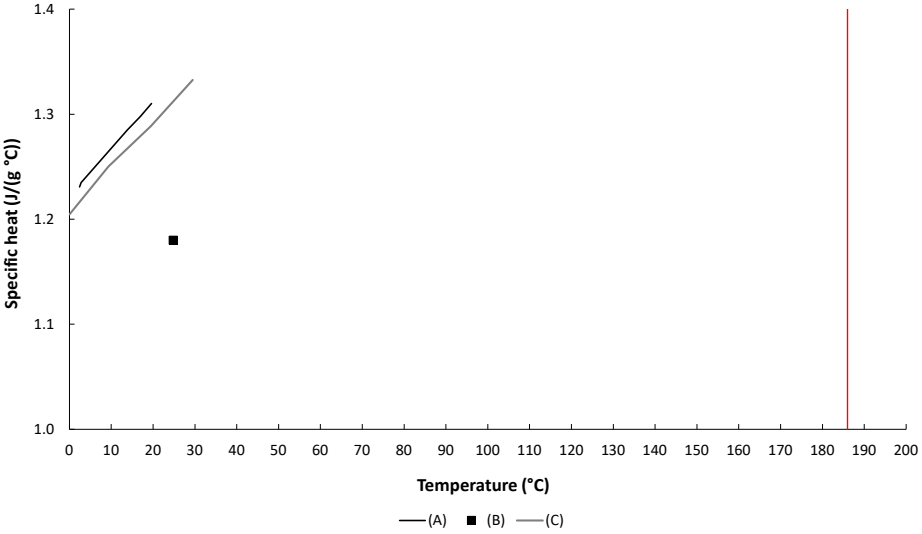

Figure 9: Specific heat values of **dulcitol** collected from literature as a function of temperature: (A) [132]; (B) [143]; (C) [71]. The red vertical line indicates the melting temperature and delimits the solid phase (left) from the liquid phase (right).

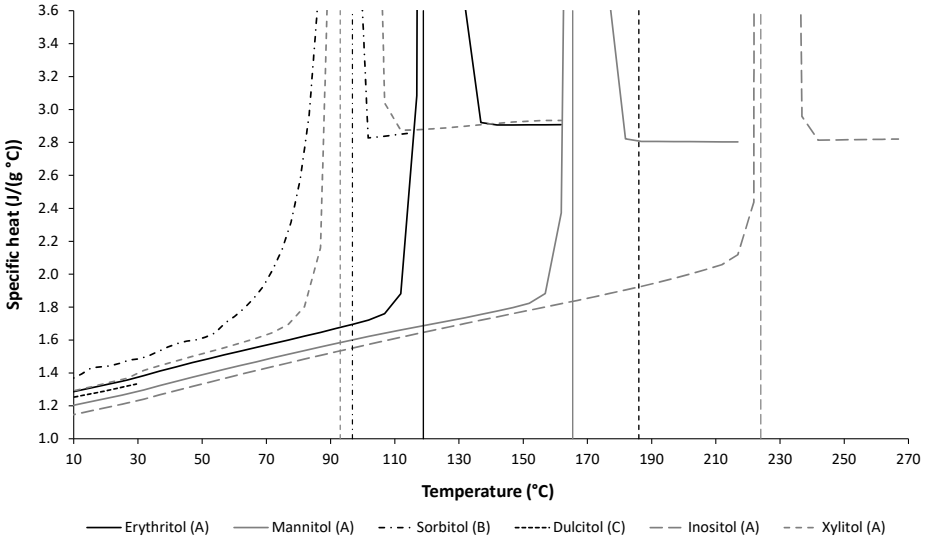

Figure 10: Comparison between the literature specific heat values of the analyzed SAs as a function of temperature: (A) [83]; (B) [92]; (C) [71]. The vertical lines indicate the melting temperatures and delimit the solid phase (left) from the liquid phase (right).

a limited number of c_{p} values only for its solid phase were found. Instead, most of the literature works reported the c_{p} of erythritol and mannitol for liquid and solid phases. In addition, the values for their supercooled liquid phase were reported by different sources. Some data in supercooled liquid phase were also found for xylitol, sorbitol, and inositol. In general, these figures show a good agreement between the c_{p} values for the studied SAs collected from different sources. Only a slightly higher discrepancy can be seen for the data of erythritol and mannitol in the supercooled liquid phase. Finally, as also evident in Figure 10, it is possible to note that the values and the behaviors of c_{p} for these SAs (except dulcitol) are very similar both in the liquid and solid phases.

3.3. Thermal conductivity

This subsection presents the values of thermal conductivity (λ) for the analyzed SAs collected from the literature. Only the works providing λ data (both regressed and experimental) associated with the corresponding temperatures were selected. Most of these λ data were obtained by performing transient hot

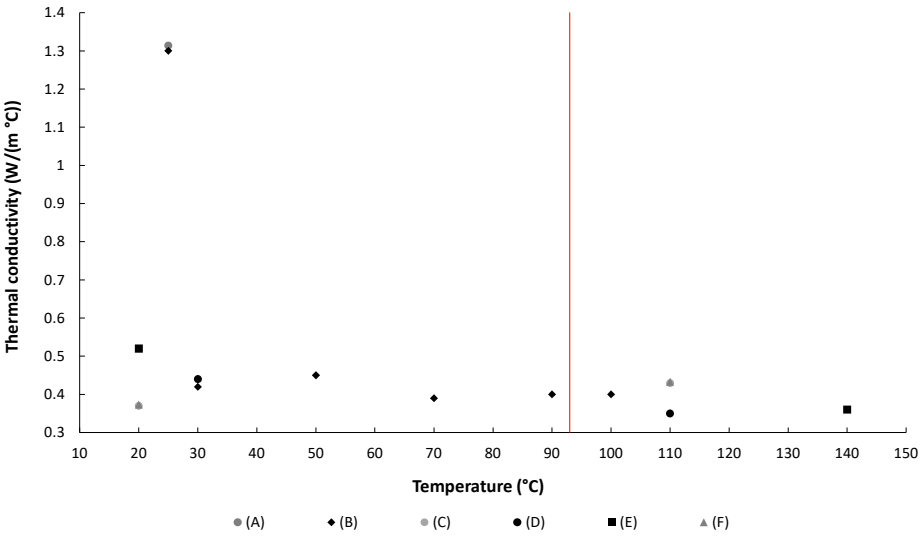

Figure 11: **Xylitol** thermal conductivity values collected from literature as a function of temperature: (A) [58]; (B) [54]; (C) [130]; (D) [77]; (E) [84]; (F) [146]. The red vertical line indicates the melting temperature and delimits the solid phase (left) from the liquid phase (right).

disk measurements. The selected values for xylitol and erythriol in their liquid and solid phases are reported in Figure 11 and Figure 12, respectively, as a function of the temperature.

As illustrated in Figure 11, a limited number of works reporting λ data of xylitol are available in the literature. Among them, only Zhang et al. [54] presented measurements in supercooled liquid phase. In addition, while the collected measurements in the liquid phase are consistent, a clear disagreement in the solid phase between the data provided by del Barrio et al. [58] and Zhang et al. [54] and the values reported in the other works [130, 77, 84, 146] is observed. Figure 12 shows a general good agreement between the literature liquid λ values of erythritol and a high discrepancy between the data in the solid phase.

Three experimental data of λ for mannitol measured at room temperature were found: 1.319 W/(m°C) [58], 1.308 W/(m°C) [153], and 1.328 W/(m°C) [111]. For sorbitol, only the measurements in the solid phase reported by Liu et al. [154] were collected. The authors showed that the λ ranged between

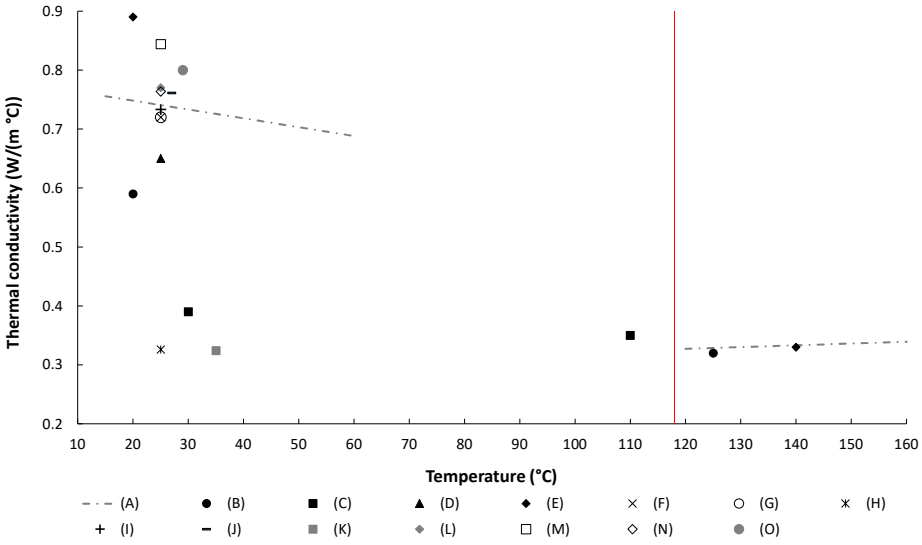

Figure 12: **Erythritol** thermal conductivity values collected from literature as a function of temperature: (A) [147]; (B) [130]; (C) [77]; (D) [100]; (E) [84]; (F) [148]; (G) [138]; (H) [149]; (I) [150]; (J) [58]; (K) [101]; (L) [151]; (M) [152]; (N) [96]; (O) [140]. The red vertical line indicates the melting temperature and delimits the solid phase (left) from the liquid phase (right).

0.400–0.445 W/(m°C) at about 23 °C. No experimental λ values for inositol and dulcitol were found in the literature.

Finally, it is important to note that the collected values of λ proved that, as well as other organic PCMs [5, 7], SAs are characterized by low thermal conductivity. Different studies analyzed the possibility to enhance λ of PCMs, including SAs, by using different techniques [155, 156, 157]. In particular, composite PCMs based on four SAs (i.e., sorbitol [154], erythritol [148, 138, 150, 151, 149, 158, 159, 82], and mannitol [153, 160]), obtained either by the absorption of the SAs into the pores of a supporting material or by adding a small amount of a material with high λ into the SAs, were analyzed. Table 10 summarizes the results of some of the main works reporting experimental λ values for the composite PCMs based on SAs. From this table, it is evident that λ of the analyzed composite PCMs are higher than that of pure SAs.

Table 10: Comparison of experimental thermal conductivity values of pure SAs (λ_{SA}) and their composite PCMs (λ_{comp}) available in the literature (as a function of temperature), together with the technique used to prepare the composite PCMs. The letters (l) and (s) indicate the liquid and solid phases, respectively.

λ_{SA} (W/(m°C))	ΔT_{SA} (°C)	Composite PCM	λ_{comp} (W/(m°C))	ΔT_{comp} (°C)	Used technique	Ref.
sorbitol						
-	-	SA-Au nanocomposites (0.002-0.0004 wt%)	0.425-0.445 (s)	23	Addition	[154]
erythritol						
0.324	35	Sepiolite (44 wt%)-SA	0.373	35	Vacuum impregnation	[101]
		SA-Sepiolite-exfoliated graphite nanoplatelets (8 wt%)	0.756	35		
0.314	-	Graphene Oxide (3wt%)-SA	0.692	-	Encapsulation	[107]
		SA-Graphene Oxide (3 wt%)-carboxymethyl cellulose (0.7 wt%)	0.699	-		
0.720	25	SA–graphite foam (25 wt%)	3.770	25	Impregnation	[138]
0.733	r.t.[a]	SA-expanded graphite (15 wt%)	4.720	r.t.[a]	Dispersion	[150]
0.733	r.t.[a]	SA-porous nichel (15 wt%)	11.60	r.t.[a]	Vacuum impregnation	[161]
0.780	29	SA-Ultrathin graphite hybrid Foam (1.8 wt%)	2.260	29	Impregnation	[140]
		SA-Ultrathin graphite hybrid Foam (1.8 wt%)-carbon nanotubes (0.8%)	4.090	29		

Continues to the following page

Continues from the previous page

λ_{SA} (W/(m°C))	ΔT_{SA} (°C)	Composite PCM	λ_{comp} (W/(m°C))	ΔT_{comp} (°C)	Used technique	Ref.
0.770	25	SA-Short carbon fibers C25 (10 wt%)	3.910	25	Addition	[151]
0.326	r.t.[a]	SA-Expanded graphite (4 wt%)	1.147	r.t.[a]	Addition	[149]
0.700	-	SA-surface roughened hydrophilic metal foam	4.500	-	Impregnation	[158]
0.730	-	SA-metal-graphene network (6 vol%)	1.900	-	Inclusion	[159]
0.733	-	SA-graphene nanoparticles (1 wt%)	1.122	-	Dispersion	[162]
mannitol						
1.308	r.t.[a]	SA-Copper oxide nanocomposite (0.5 wt%)	1.637	r.t.[a]	Dispersion	[153]
0.600	-	SA-expanded graphite (15 wt%)	7.320	-	Addition	[163]
1.320 (s)	-	SA-graphene nano plates (5 wt%)	3.100 (s)	-	Dispersion	[160]
0.600 (l)	-		2.300 (l)	-		

[a] Room temperature

3.4. Other properties

A very limited number of literature sources reporting experimental values of dynamic viscosity (μ), liquid density (ρ_l) and solid density (ρ_s) with corresponding temperatures were found. The collected data of these properties for the analyzed SAs are provided in Table 11, along with the corresponding temperature ranges. From Table 11, it is evident that only few works presenting the measurements of density and viscosity for five SAs were found. Instead, no data for sorbitol were collected. In particular, the collected values of density show that the percentage volume changes between the solid and liquid phases are about 15 % for xylitol and 13 % for erythritol. These values should be taken into account for the design of suitable LHTES systems. In addition, Table 11 shows that xylitol has higher μ values than those of the other SAs, especially at low temperatures. Since a relevant barrier for nucleation and a limited mobility of the molecules are due to high viscosity values, this could partially explain the significant and stable supercooling of xylitol [58, 54, 164]. Finally, it is important to note that the μ values of Table 11 collected from Shao et al. [164] correspond to measurements at high shear rate, where the analyzed materials show a Newtonian behavior. In this case, the temperature behavior of the viscosity agrees with the Arrhenius model. However, it was also shown that these SAs are non-Newtonian fluids at shear rates lower than their critical shear rates [164, 59].

Table 11: Experimental values of density in the liquid (ρ_l) and solid (ρ_s) phases and viscosity (μ) for the studied SAs available in the literature as a function of temperature.

$\Delta\rho_s$ (kg/m^3)	ΔT of ρ_s (°C)	$\Delta\rho_l$ (kg/m^3)	ΔT of ρ_l (°C)	$\Delta\mu$ (Pa s)	ΔT of μ (°C)	Reference
xylitol						
1500.1–1472.5	30–90	-	-	10.01[a]–0.4127	57–96	[58]
1497.1–1477.0	30–90	1374.6[a]–1311.5	40–130	68.05[a]–0.2441	40–108	[54]
1505.0–1487.7	20–90	1344.6–1324.4	120–150	-	-	[84]
-	-	-	-	0.5	90	[76]
-	-	-	-	4.369[a]–0.0146	63–173	[164]
erythritol						
1490.0–1427.0	30–110	-	-	0.0748–0.0293	121-134	[58]
1440.4–1436.2	20–118	1289.1–1273.8	120-150	-	-	[84]
-	-	-	-	0.0822[a]–0.0056	99–189	[164]
mannitol						
1493.6–1394.6	30–150	-	-	0.0806[a]–0.0100	120-150	[58]
-	-	-	-	0.1218[a]–0.0079	141–236	[164]
inositol						
-	-	-	-	0.1687[a]–0.0424	210–275	[164]
dulcitol						
-	-	-	-	0.0469[a]–0.0057	162–257	[164]

[a] supercooled liquid

4. Thermal stability

In this section, a literature survey of the works reporting thermal stability tests for SAs is reported. In particular, the following studies were collected and analyzed: the works reporting the results obtained by keeping SAs at constant temperatures for a defined time to study their thermal endurance; the studies presenting their degradation temperatures measured with the TGA technique; the works providing the results for cycling stability analyses. Moreover, new TGA measurements performed on the analyzed SA samples are presented.

4.1. Thermal endurance

Brief descriptions of the collected literature works presenting thermal endurance tests for the analyzed SAs are reported in this section. As can be seen, there are lots of works dedicated to mannitol, while several papers provide comparisons among the considered SAs. No tests were found for sorbitol.

4.1.1. Erythritol

Recently, Alferez Luna et al. [165] investigated the thermal endurance of erythritol kept at different constant temperatures above its T_{m}, both under ambient air and inert atmosphere (and with and without antioxidant), for several hours. In particular, the authors performed tests where the samples were kept at 121 °C, 131 °C, and 141 °C for a maximum of 100 hours and others where the samples were kept at 141 °C for 935 hours. From the DSC measurements carried out on samples before and after the heat treatment, it was found a decrease of ΔH_{m} of erythritol under air as the temperature of the heat treatment increased. The results also showed: a degradation rate of the erythritol mixed with antioxidants lower than that of pure erythritol under ambient air; lower ΔH_{m} reductions in experiments under argon atmosphere than those under ambient air. In the tests under ambient air, the authors also observed the browning of erythritol samples and suggested that it could be related to oxidation/dehydration processes. Instead, the samples with antioxidant heated under ambient air darkened less than the samples of pure erythritol. Moreover, it was noted that some erythritol

samples remained liquid and underwent a glass transition. The samples of pure erythritol under an argon atmosphere barely changed color and no browning of the sample of erythritol-antioxidant under argon was observed. In addition, all the samples solidified at room temperature. Among the different samples subjected to heating treatment for 100 hours, the samples of pure erythritol under ambient air showed the highest mass loss rate due to oxidation. However, the addition of the antioxidant to erythritol exposed to ambient air helped to reduce the mass loss during oxidation. The FTIR measurements showed the presence of carbonyl groups and conjugated carbonyl compounds after heat treatment for erythritol under air; instead, they proved the chemical stability of erythritol under argon up to 141 °C. Moreover, the authors also found a good thermal stability of pure erythritol under argon atmosphere up to 935 hours of heat treatment.

4.1.2. Mannitol

Solé et al. [166] tested the thermal endurance of d-mannitol to evaluate the effect of oxygen by placing different sample masses (250 mg, 500 mg, 750 mg, and 1000 mg) in an oven at a constant temperature of 190 °C for two days. The heated samples showed significant changes in color: the sample with the smaller mass showed a dark brown color, while the heavier samples presented a lighter brown color with increasing sample mass. It was stated that this effect could be due to the oxygen gradient along the sample. To check if the color changes were also reflected in the chemical structure, the authors performed FTIR measurements on the heated samples. The results showed that the peak giving a hint of oxidation was detected only for the smaller sample, although all samples changed color. Therefore, it seemed that the strongest oxidation was shown by the smaller sample. By comparing the results of the FTIR analysis with those obtained by Burger et al. [167], the authors concluded that, after being heated in the oven, all the samples changed their polymorphic phase with respect to that of the fresh sample.

Sagara et al. [168] analyzed the thermal endurance of pure d-mannitol and d-mannitol impregnated into nanosized pores of porous SiO_2 grains. To evaluate their thermal degradation characteristics by means of the constant temperature kinetics, a DSC was used to measure the latent heats of the samples placed in closed crucibles under an inert atmosphere which were maintained at specific constant temperatures higher than their T_m for several hours. As indicated by the time-dependent degradation ratio of its ΔH_m, d-mannitol has a short life span as a PCM due to high thermal degradation. On the other hand, at a retention temperature 10 K higher than its T_m, the thermal degradation period of the d-mannitol/SiO_2 composite with average pore size of 11.6 nm was 13 times longer than that of pure d-mannitol.

Rodríguez-García et al. [169] analyzed the thermal endurance of d-mannitol by keeping different samples of about 20 g at 180 °C for different periods of time under inert atmospheres (argon or nitrogen) at a pressure up to 0.1 MPa. They observed a progressive browning of the sample, a change in consistency from hard solid to soft paste, and a decrease in mass. In particular, the d-mannitol sample had a brown color after 72 hours and a dark brown color after 122 hours; instead, after 171 hours and 268 hours, a dense brown syrup that did not crystallize was obtained. The sample tested in nitrogen atmosphere showed a smaller mass loss than that of the sample analyzed in argon atmosphere. However, the mass loss and the degradation of the heated sample clearly indicated the production of a large amount of volatile species during heating. In addition, the Vis-UV spectra of the heated samples seemed to indicate that the degradation reactions in different atmospheres could proceed differently, even if the species responsible for the browning of the sample are apparently the same, regardless of the atmosphere used during the melting of the sample. Since d-mannitol suffered not only mass loss but also strong browning even under inert atmospheres, the authors deemed that its thermal degradation is more likely to be related to the caramelization process than to the oxidation process, as instead stated elsewhere [166]. Based on their results, the authors inferred that the d-mannitol cannot be considered feasible as PCM even under inert atmosphere. Moreover,

they stated that there might be a correlation between its thermal endurance and the number of thermal cycles, proving that the cycling stability tests do not provide reliable description of the long-term durability of d-mannitol.

To verify its feasibility as PCM in a commercial LHTES system, Bayón and Rojas [170] studied the thermal endurance of d-mannitol by keeping molten samples of about 30–40 g at 180 °C in ambient air for different time periods (up to 16 days). The authors observed that the sample mass strongly decreased and it changed its appearance into a sticky dark brown paste. It was explained that these results indicate that d-mannitol suffer thermal degradation due to caramelization processes which produce a large amount of volatile and non-volatile species during heating. Moreover, in agreement with Rodríguez-García et al. [169], it was pointed out that the results of the cycling stability tests usually reported in the literature are misleading because the measurement conditions are not representative of the PCM behavior under real working conditions. In conclusion, the authors stated that d-mannitol undergoes severe degradation at temperatures close to its T_{m} not only under ambient air but also under inert atmosphere and should be removed from the lists of PCM candidates for any LHTES applications.

Neumann et al. [171] analyzed the thermal endurance of d-mannitol by keeping samples of about 350 mg in ambient air at three temperatures above its T_{m} for about 5 days. The DSC and FTIR measurements performed on the heated samples proved that d-mannitol tends to degrade if maintained for several hours at constant temperatures above its T_{m}. In fact, it was found a decrease of its melting enthalpy, an increase in mass loss over time, and the formation of aldehydes and ketones in an oxidation reaction detected by the change of sample color over time. However, the authors found an improvement of its thermal stability by adding antioxidants to d-mannitol in the presence of ambient air. An even greater thermal stability improvement was obtained by replacing air with argon. However, it was shown that the combination of antioxidants and argon, while improving stability, did not completely stopped the degradation. Furthermore, under argon atmosphere the degradation rate did not seem to

depend on the retention temperature. The authors concluded that, although the addition of antioxidants and the exposure to inert atmosphere improve its thermal stability, it does not seem possible to use d-mannitol as PCM without any degradation of the melting enthalpy; therefore, the possibility to use d-mannitol as PCM in specific applications depends on the required number of storage cycles and on the specific retention temperatures above T_{m}.

4.1.3. Comparison between sugar alcohols

The degradation of erythritol, xylitol, and mannitol samples kept at 40 K above their melting temperatures for two hours was examined by Zhang et al. [134]. The authors noted that their thermal properties changed during this process, particularly their latent heat of fusion, and these SAs became tanned. In particular, T_{m} and ΔH_{m} of erythritol decreased from 119.4 to 114.3 °C and from 338.7 to 271.6 kJ/kg, respectively. While its T_{m} slightly increased from 95.1 to 96.0 °C, ΔH_{m} of xylitol decreased from 251.4 to 231.7 kJ/kg. T_{m} and ΔH_{m} of mannitol decreased from 166.9 to 164.0 °C and from 296.1 to 248.1 kJ/kg, respectively. Therefore, the ΔH_{m} values of erythritol, xylitol, and mannitol reduced by 19.8 %, 7.8 %, and 16.2 %, respectively.

Nomura et al. [60] investigated the thermal endurance of the following three SAs: mannitol, dulcitol, and inositol. By using the same measuring method of the above described work [168], they assessed the thermal degradation characteristics of the studied SAs by the constant temperature kinetics based on latent heat values of each PCM measured by a DSC. The results showed that, despite mannitol and dulcitol have a similar molecular structure and therefore potentially similar degradation systems, the degradation rate of mannitol was lower than that of dulcitol. Instead, in the case of inositol, although its melting temperature is higher than that of mannitol and dulcitol, its degradation rate was lower than that of the other two SAs. It was concluded that this indicates a higher thermal resistance of some ring-structured alcohols, such as inositol, compared to sugar alcohols with a linear chain structure, such as mannitol and dulcitol.

The thermal endurance of four SAs (i.e., erythritol, d-mannitol, inositol, and d-dulcitol) was analyzed by Shao et al. [32]. The tests for erythritol were carried out by keeping samples of about 10 g at constant temperatures between 5 and 65 °C above its T_{m} for up to twenty hours. Instead, the samples of the other SAs were kept at the following temperatures for up to ten hours: temperatures between 5 and 35 °C above T_{m} of d-mannitol and d-dulcitol and temperatures between 5 and 20 °C above T_{m} of inositol. From the DSC measurements, the authors observed the degradation of T_{m} and ΔH_{m} of the analyzed sugar alcohols which was faster with a higher degree of superheating. Among the studied SAs, erythritol showed the best thermal resistance compared to the others. The results of the FTIR measurements performed on samples exposed to ambient air showed that the analyzed SAs were subject to oxidation and generated ketones and aldehydes during heating treatment. Moreover, the authors have verified the possibility to improve their thermal stability by effectively suppressing oxidation introducing an inert protective atmosphere. In particular, the results showed that the duration for a decay of 10 % of ΔH_{m} for inositol could be extended by 9 times using nitrogen atmosphere. However, it was also pointed out that, at high temperatures in an inert atmosphere, other complex reactions may still occur and the analysis of these reactions may allow further improvements in the thermal endurance of the SAs analyzed. Finally, the authors stressed the importance of carefully controlling the heating temperatures and its duration to slow their thermal degradation and to delay the off-design operation conditions of the LHTES systems.

4.2. Degradation temperature

Table 12 presents the literature degradation temperature measurements for the studied SAs carried out with the TGA technique, together with new values measured by our research group. The maximum thermal stable temperature, T_{max} (i.e., the maximum temperature at which the substance can be heated with negligible loss of mass), and the final degradation temperature, T_{deg} (i.e., the temperature at which the substance is completely evaporated), are provided. In

our measurements, the values of T_{max} and T_{deg} refer to the achievement of a mass loss of 1 % and 95 %, respectively. The purge gas and the heating rate used during the thermogravimetric analysis are also provided in Table 12.

Figure 13 depicts the percentage mass for the measured sugar alcohols as a function of the temperature. As can be seen from Figure 13, in all the analyzed SAs, the loss of mass occurs in a single step. From this figure, the initial onset temperature values, $T_{onset,i}$ (i.e., the temperature obtained from the intersection of the tangents to the point of deviation from the initial weight and to the inflection point of the TG curve of each sugars), were also calculated according to the standards [172]. This temperature is equal to 314.0 °C for xylitol, 352.4 °C for sorbitol, 303.2 °C for erythritol, 363.9 °C for mannitol, 377.1 °C for inositol, and 365.9 °C for dulcitol.

From Table 12, it can be seen that there are several studies where the authors performed thermogravimetric analysis for erythritol, mannitol, xylitol, and dulcitol, while a very limited number of results were collected for sorbitol and inositol. As a general comment, the T_{max} for the six SAs are on average equal to about 200 °C for xylitol, about 250 °C for sorbitol, slightly lower than 200 °C for erythritol, about 250 °C for mannitol, lower than 300 °C for inositol, and about 250 °C for dulcitol. It can be noted that the difference between T_{max} and T_m is about 60 °C for dulcitol, about 89 °C for erythritol, mannitol, and inositol, and more than 100 °C for xylitol and sorbitol. Therefore, to proper use them in LHTES applications, it should be taken into account the specific maximum temperatures that these SAs can be brought with respect to their T_m. However, it should be noted that the values reported for the same SA are in some cases very different. This may be due to the type of instrumentation, the purging gas used during the test, the purity of the sample, the ramping rate, and the choice of mass loss values associated with T_{max} and T_{deg}.

As concerns the last point, it is worthwhile pointing out that only a very limited number of works report details about the mass loss values associated with these temperatures. In this regard, Salyan and Suresh [173] and Salyan et al. [110] explained that the reported T_{max} for mannitol (equal to 300 °C)

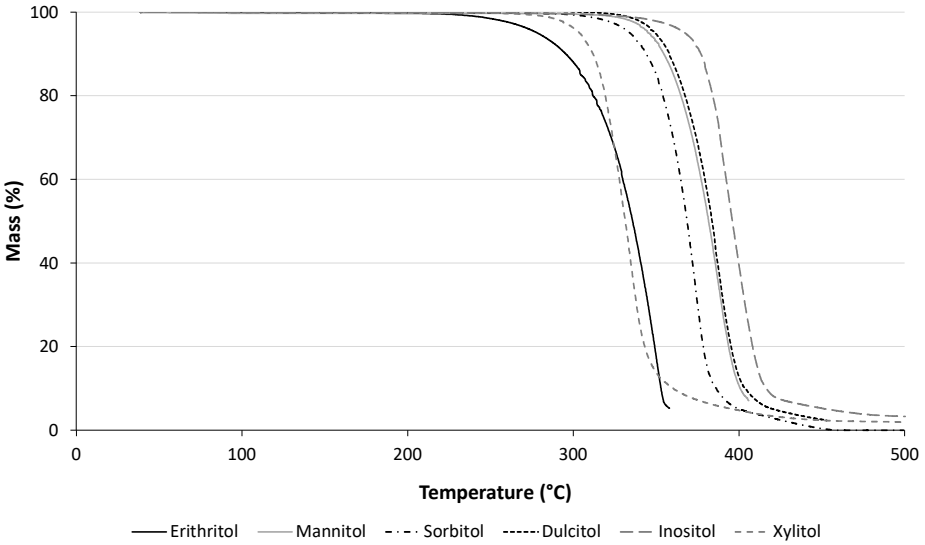

Figure 13: TG curves of erythritol, mannitol, sorbitol, dulcitol, inositol, and xylitol.

corresponds to a mass loss of less than 2%. Instead, John et al. [174] reported a $T_{\max}$ of 190 °C for dulcitol, corresponding to a mass loss lower than 1%. Salyan and Suresh [153], Salyan and Suresh [175], and Pethurajan et al. [111] reported a $T_{\deg}$ of 500 °C for mannitol, corresponding to a residual mass of 2.84 %. The $T_{\deg}$ of 557 °C for mannitol measured by Mojiri et al. [142] corresponds to a residual mass of 0.172 %.

Finally, some studies reported TGA measurements performed on cycled mannitol. In particular, Salyan and Suresh [175] found a degradation temperature of around 290 °C for mannitol after 100 cycles. Salyan and Suresh [173] showed that, after 350 cycles, mannitol was stable up to a temperature of 240 °C. Salyan et al. [110] reported that, after 1000 cycles, the analyzed sample of mannitol showed a narrow window of decomposition temperature and the decomposition trigger was at 240 °C.

Table 12: Measurements of maximum thermal stable temperature ($T_{\max}$) and final degradation temperature ($T_{\deg}$) for the studied SAs carried out with TGA at various heating rates (HR).

$T_{\max}$ (°C)	$T_{\deg}$ (°C)	HR (°C/min)	Purge gas	Reference
xylitol				
200.0	330.0	10	air	[76]
178.1	402.2	10	nitrogen	[86]
-	359.5	10	nitrogen	[87]
200.0	-	10	argon	[81]
200.0	328.2	10	nitrogen	[82]
278.6	395.3	20	nitrogen	this work
sorbitol				
256.4	491.4	10	nitrogen	[92]
240.0	-	10	argon	[81]
307.1	399.6	20	nitrogen	this work
erythritol				
183.7	250.0	3	nitrogen	[147]
180.0	255.0	5	argon	[98]
160.0	-	5	argon	[81]
240.0	335.0	10	nitrogen	[176]
203.6	309.2	10	-	[135]
180.0	300.0	10	nitrogen	[101]
240.0	335.0	10	nitrogen	[102]
200.0	318.0	10	nitrogen	[177]
-	326.2	10	nitrogen	[87]
238.2	358.0	20	nitrogen	this work
215.0	316.0	-	-	[107]
mannitol				
267.0	427.0	5–25 [a]	nitrogen	[141]
259.0	424.0	10	air	[9]
294.0	410.0	10	nitrogen	[176]
235.6	312.5	10	nitrogen	[178]
207.0	557.0	10	nitrogen	[142]

Continues to the following page

Continues from the previous page

T_{max} (°C)	T_{deg} (°C)	HR (°C/min)	Purge gas	Reference
300.2	397.0	10	nitrogen	[179]
252.0	386.0	10	nitrogen	[113]
280.0	360.0	10	nitrogen	[115]
50.0	340.0	10	nitrogen	[112]
300.0	-	10	nitrogen	[61]
280.0	-	10	argon	[81]
270.0	-	10	air or argon	[170]
300.0	500.0	20	-	[153]
300.0	380.0	20	nitrogen	[173]
323.0	405.8	20	nitrogen	this work
208.9	500.0	-	nitrogen	[111]
310.0	500.0	-	-	[175]
300.0	-	-	-	[110]
inositol				
271.6	526.7	10	dry air	[117]
323.1	456.5	20	nitrogen	this work
dulcitol				
190.0	-	2	nitrogen	[174]
293.0	481.0	10	air	[9]
263.5	349.5	10	nitrogen	[178]
202.0	312.0	10	air	[70]
295.0	-	10	nitrogen	[61]
332.1	420.3	20	nitrogen	this work

[a] The values of the temperatures are slightly different depending on the various heating rates from 5 to 25 °C/min

4.3. Cycling stability

In this section, both studies reporting detailed results of the thermal cycling tests of the selected SAs and the works providing only a qualitative description of the results have been selected and analyzed. It is important to point out that, although measurements of other thermal properties for the cycled samples and/or FTIR measurements to evaluate their chemical stability were reported in various works, this review focused on the results regarding the phase change properties of the cycled SAs. Table 13 shows the values of melting and crystallization thermal properties for the cycled SAs measured with a DSC, together with the available sample masses and the equipments for cycling the samples.

Table 13: Melting temperature (onset) (T_m), latent heat of melting (ΔH_m), crystallization temperature (onset) (T_c), and latent heat of crystallization (ΔH_c) for the cycled SAs measured with a DSC. The equipments used for cycling the samples and the measured masses are also reported.

Cycles	T_m (°C)	ΔH_m (J/g)	T_c (°C)	ΔH_c (J/g)	Equipment	Mass (g)	Reference
erythritol							
1	118.7	357.3	19.2	141.8	DSC	-	[99]
10	118.5	354.3	15.8	57.7			
1	118.4	339.3	-	-	DSC	0.019	[180]
20	114.4	313.8	-	-			
1	119.2	-	33.0	213.1	DSC	-	[181]
20	105.4	-	46.2	221.3			
1	127.5	311.0	53.1	308.2	heater and	-	[97]
100	127.0	331.4	51.3	308.0	cooling water bath		
1	118.6	349.9	33.9	224.2	hot plate heater	-	[100]
100	118.6	349.8	36.4	155.8			
1	118.1	340.6	38.8	252.3	drying oven	-	[95]
100	118.2	332.3	38.8	250.2			
1	119.0	349.9	33.5	224.2	drying oven	-	[107]
100	118.9	349.8	36.2	155.8			
1	117.0	339.0	-	-	oven	200	[182]
100	122.0	340.0	-	-			
500	106.0	312.0	-	-			
1000	119.0	305.0	-	-			
mannitol							
1	151.0	234.4	114.1	224.6	DSC	0.005–0.008	[108]
50	131.9	99.5	62.5	109.5			
1	168.8[a]	284.9	107.7[a]	214.4	furnace	20–30	[114]
50	164.0[a]	141.0	99.0[a]	156.0			
1	166.4	281.9	120.2	219.5	hot plate heater	25	[153]

Continues to the following page

Continues from the previous page

Cycles	T_m (°C)	ΔH_m (J/g)	T_c (°C)	ΔH_c (J/g)	Equipment	Mass (g)	Reference
50	165.9	256.2	119.9	252.0			
100	166.4	241.2	118.2	207.4			
1	165.0	317.0	117.0	255.0	DSC	-	[183]
100	165.0	297.0	126.0	265.0			
1	165.3	282.0	123.0	241.3	hot plate heater	50	[111]
100	167.7	280.2	123.5	238.6			
1	168.4[a]	281.9	118.6[a]	219.5	hot plate heater	50	[175]
100	168.5[a]	241.2	116.3[a]	207.4			
1	166.9	281.9	120.2	219.5	hot plate heater	50	[173]
350	165.6	225.4	119.6	187.3			
1	166.4	281.9	120.2	219.5	hot plate heater	250	[110]
1000	164.3	209.3	118.8	165.2			
inositol							
1	216.3	185.3	182.3	206.6	DSC	0.005–0.008	[108]
50	214.9	167.5	160.9	165.5			
1	225.5	351.6	185.7	325.8	hot plate heater	30	[116]
50	223.4	220.4	182.4	200.1			
1	225.5[a]	351.6	-	-	hot plate heater	30	[184]
50	229.9[a]	210.1	-	-			

[a] peak temperature

From Table 13, it can be seen that various studies reporting systematic analyses for the long-term thermal stability of erythritol and mannitol are available in literature. Instead, a very limited number of data sources were found for inositol. It is worthwhile pointing out that procedures characterized by different equipments to cycle the samples, cycling methods, number of cycles, temperature ranges, sample atmospheres, and sample masses and purities were used to carry out the cycling stability tests reported in this table. Consequently, this could be the reason behind the differences between the collected values. However, from the values reported in Table 13, it can be noted that, although lower melting properties were generally measured for the cycled samples of all three SAs, the cycling stability of mannitol and inositol seems lower than that of erythritol.

Because of their general low cycling stability, many of the analyzed studies concluded that the studied SAs cannot be considered as good PCMs for different LHTES applications, unless specific methods to enhance their thermal stability are taken into account. Consequently, specific stabilization processes to improve their long-term thermal stability have been proposed and evaluated. For erythritol, the following stabilization processes have been studied: the dispersion of nanoparticles into this SA [97, 95], the development of PCM composites comprised of this SA [185, 77, 186, 101, 177, 107, 187], and the use of the encapsulation method [100]. There are also some works regarding the stabilization processes for mannitol [153, 175, 173, 110, 111, 112] and inositol [184, 116].

4.3.1. Erythritol

Despite the degradation of its thermal performance was usually found in the considered works, the analyzed results of the cycling performance tests for erythritol showed a significant discrepancy between the melting and crystallization properties. Starting from the tests characterized by a limited number of cycles (lower than 100), a decrease of T_{m} and ΔH_{m} was measured by Agyenim et al. [180] after 20 cycles. A decrease of T_{m} after 20 cycles was also observed by Karthik et al. [138] and Shobo et al. [181]. Instead, due to its supercooling,

the crystallization point measurements obtained by these authors after 20 cycles were higher than those measured in the first cycle. In contrast, as shown in Table 13, the results presented by Zeng et al. [99] showed that the values of T_m and ΔH_m were stable after 10 cycles; however, a severe decrease of T_c and ΔH_c was observed. The results reported by Tan et al. [101] also proved that its crystallization properties drastically decreased after 10 cycles, proving that its supercooling was unstable. Moreover, Yuan et al. [188] showed that the difference between the measured values of T_m and T_c for erythritol increased after 40 cycles. Other works [186, 185, 177] reported a significant degradation of its thermal performance after only 5 cycles, with a decrease of the latent heat of more than 40 % in same cases. On the other hand, Puupponen et al. [77] analyzed the cycling stability of erythritol by performing 10 DSC cycles and they did not find a significant variation of its phase change properties upon the longer cycling. The cycling stability results for erythritol obtained after 100 cycles (Table 13) show that the values of T_m and ΔH_m were usually stable, while a decrease of T_c and ΔH_c was found only in two cases [100, 107]. It is worthwhile pointing out that the ΔH_m values collected by Vivekananthan and Amirtham [97] are not in agreement with the behavior reported in the figures of the their work and the statements of the authors. Despite it is not confirmed by the selected data, the authors explained that cycled erythritol presented a clear decrease of its ΔH_m, as shown in the figures, and a degradation of the thermal-physical properties. Finally, it is important to note that only a slightly decrease of T_m and ΔH_m was observed by Shukla et al. [182] after 1000 cycles.

4.3.2. Mannitol

Unlike erythritol, the values reported in Table 13 for mannitol show that it has a clear degradation of its thermal performance. However, it possible to note that the decrease of the melting and crystallization properties obtained by Solé et al. [108] and Bayón and Rojas [114] after 50 cycles is much higher than that measured in the works that performed a higher number of cycles (at least 100 cycles). This could be due to the fact that the tests were performed by using

various procedures characterized by different measurement conditions. Also the following literature studies showed the degradation of the thermal performance of mannitol after a certain number of cycles, but a certain discrepancy between their results emerged since different measurement procedures were used. The DSC measurements carried out by Solé et al. [166] and Gasia et al. [9] after 50 cycles and 100 cycles, respectively, showed a decrease of its latent heat of more than 50 % in both cases. He et al. [112] showed that a decrease of its latent heat was evident after 10 cycles and the DSC results presented two peaks in the heating phase probably due to its polymorphism. Barreneche et al. [66] also showed that mannitol could solidify as different solid phases after few thermal cycles for the same reason. A clear change of the melting properties of mannitol was observed by Rodríguez-García et al. [169] after 50 cycles performed in inert atmospheres (argon and nitrogen atmospheres). The results obtained by Miró et al. [189] performing a cycling stability test showed that mannitol had high melting and crystallization latent heats (over 200 kJ/kg) even after 50 cycles, although its storage capacity seemed to decrease a bit with the cycles. Although their DSC measurements for mannitol showed two peaks during the heating phase with thermal cycling, a limited decrease of its ΔH_{m} was seen by Mojiri et al. [142] after 100 cycles. Neumann et al. [190] presented a comparison between the results for mannitol obtained by carrying out 7 and 20 cycles in a DSC in different atmospheres. The results of these cycling stability tests showed that the value of ΔH_{m} significantly decreased for the sample in contact with oxygen (almost 38 %), decreased less for the sample in vacuum, and was almost constant for the sample in nitrogen atmosphere. Moreover, the authors reported the results obtained after 500 cycles for sample measured in a nitrogen atmosphere, showing that its ΔH_{m} decreased of about 9 %. Besides the results of the cycling performance test reported in Table 13, Stathopoulos et al. [183] analyzed the long-term thermal performance of mannitol macro-encapsulated in spheres. They studied three spheres characterized by different sealing methods to have small, minor, and no exposure to ambient air. After 60 cycles, a smaller decrease of ΔH_{m} and ΔH_{c} of the sample occurred in the sphere with

no exposure to air with respect to that of the other spheres. However, a decrease of 24.5 % and 16 % for ΔH_{m} and ΔH_{c}, respectively, was also obtained in this case. It is worthwhile pointing out that many of the analyzed studies [108, 114, 153, 175, 190, 183] explained that the color of the measured samples turned from white to brown with thermal cycling in ambient air. This can be a hint for its degradation due to oxidation. In particular, Stathopoulos et al. [183] stated that the degradation of mannitol is highly influenced by the presence of ambient air. However, in agreement with the explanation reported in Section 4.1, Rodríguez-García et al. [169] showed a change in color of the samples cycled in inert atmospheres, proving a certain physical degradation of mannitol also in absence of oxygen. Instead, no change of color was seen by Neumann et al. [190] for the samples measured in nitrogen atmosphere.

4.3.3. Inositol

As mentioned before, few works presenting cycling stability tests for inositol using a DSC were found in the literature. As shown in Table 13, they are all characterized by the same number of cycles, showing a decrease of the melting and crystallization properties. Also the results obtained by Solé et al. [166] showed that ΔH_{m} and ΔH_{c} decreased about 10 % and 20 %, respectively, after 50 cycles.

4.3.4. Sorbitol, xylitol, dulcitol

Finally, it can be noted that no cycling stability tests for xylitol, sorbitol, and dulcitol are reported in Table 13. In fact, no literature reference presenting long-term thermal stability analysis for sorbitol were found. For xylitol, it was found only the cycling stability test presented by Zhang et al. [54] that was performed by heating the xylitol sample in a furnace and by triggering the crystallization by injecting air bubbles in the liquid sample. The results showed that ΔH_{m} of xylitol has reduced by less than 2% after twenty cycles, proving that xylitol could have good cycling performance. However, for a more accurate assessment of the cycling stability of xylitol, additional analyses characterized by

a higher number of thermal cycles could be useful. As concerns dulcitol, different works presenting cycling stability tests are available in the literature. They showed that dulcitol presented a quick and severe degradation of its thermal properties with cycles [166, 108, 174, 9]. In particular, Solé et al. [166] explained that, besides the fact that T_{m} and T_{c} of dulcitol significantly decreased when it was cycled, no exothermic peak of solidification was observed in the DSC measurements after the 19th cycle. The poor long-term thermal stability of dulcitol was also confirmed by the results presented by Solé et al. [108] and Gasia et al. [9], which showed a severe chemical degradation and the same lack of liquid-solid phase transition after a certain number of cycles. Similar outcomes were also provided by the cycling stability test performed on a bulk dulcitol sample presented by John et al. [174]. The authors explained that long-term thermal stability of dulcitol is highly influenced by the upper cycle temperature and values slightly above its melting provided the best results. In particular, a upper cycle temperature of about 200 °C ensured the thermal stability of the sample for about 90 cycles. However, it was concluded that dulcitol is stable for a too limited number of thermal cycles to be actually used as PCM in medium temperature LHTES applications, such as solar cookers.

5. LHTES systems based on sugar alcohols

In this section, the works collected from the literature that experimentally and numerically evaluated the thermal performance of SAs used as PCMs in LHTES systems are analyzed. A summary of the collected works is reported in Table 14. As can be noted, the large majority of works evaluated erythritol as PCM; as highlighted above, this is due to the fact this SA presents favorable thermophysical properties and less thermal stability issues.

Table 14: Literature works concerning SAs used as PCMs in LHTES systems.

Reference	Application type	Investigation	Mass (kg)	Measured properties	Supplier
Erythritol					
Kaizawa et al. [191]	Heat exchangers	Experimental	80	-	-
Agyenim et al. [192, 193, 180]		Experimental	20	T_{m}, ΔH_{m}	Mitsubishi Chemical, Japan
Nomura et al. [194]		Experimental	9.3-27.9	-	-
Nomura et al. [195]		Experimental	27.9-46.5	-	-
Mayilvelnathan and Arasu [162]		Experimental	8.5	T_{m}, ΔH_{m}, λ	-
Abreha et al. [196]		Experimental and numerical	50	-	-
He et al. [197]		Experimental and numerical	-	-	-
Anish et al. [198]		Experimental	1.5	-	Herbo Veda, Noida, India
Anish et al. [199, 200, 201]		Experimental and numerical	-	-	Herbo Veda, Noida, India
Sharma et al. [202]	Solar cookers	Experimental	45	-	Mitsubishi Chemical, Japan
Chen et al. [203]		Numerical	-	-	-
Lecuona et al. [204]		Experimental	-	-	-
Tarwidi [205]		Numerical	-	-	-
Unger et al. [206]		Experimental	-	-	-
Mawire et al. [207]		Experimental	5.44	-	Faithful to Nature, South Africa
Coccia et al. [74]		Experimental	2.5	T_{m}, T_{c}, ΔH_{m}, ΔH_{c}	-
Osei et al. [208]		Experimental	2.5	-	-
Anilkumar et al. [209]		Experimental and numerical	1.5-6.06	-	-

Continues to the following page

Continues from the previous page

Reference	Application type	Investigation	Mass (kg)	Measured properties	Supplier
Papadimitratos et al. [210]	Solar collectors	Experimental	4.2-7.0	-	-
Wang et al. [211, 212, 213, 214], Li et al. [215], Guo et al. [216, 217]	Mobilized TESs	Experimental and numerical	60 and 74	T_m, T_c, ΔH_m, ΔH_c	Bin Zhou San Yuan Biotechnology Co. Qing Dao, China.
Guo et al. [218]		Experimental and numerical	42.62-47.36	-	-
Xylitol					
Anish et al. [201]	Heat exchangers	Experimental	-	-	Herbo Veda Pvt., Noida, India
Anish et al. [219]		Experimental	1.2	-	-
Shon et al. [220]		Experimental	4.2	-	-
Saikrishnan et al. [85]		Experimental	-	T_m, ΔH_m	-
Coccia et al. [73]	Solar cookers	Experimental	2.5	T_m, ΔH_m	-
Mannitol					
Ling et al. [221]	Solar collectors	Experimental	14	-	-
Zhang et al. [113]		Experimental	-	T_m, T_c, ΔH_m, ΔH_c, λ, thermal stability	Aladdin Reagent (Shanghai) Co.
Kumaresan et al. [222]	Solar cookers	Experimental	51.66	-	Sisco Research Lab. Pvt., Mumbai, India
Oró et al. [223], Gil et al. [224]	Absorption cooling systems	Experimental	-	T_m, T_c, ΔH_m, ΔH_c	-
Peiró et al. [225]	Heat exchanger	Experimental	165	T_m, ΔH_m	QUIMIVITA
Sorbitol					
Beemkumar et al. [226]	Heat exchangers	Experimental	-	-	-
Beemkumar et al. [227]	Solar collectors	Experimental	-	-	-

5.1. Erythritol

Sharma et al. [202] experimentally investigated the performance of a solar cooker based on a vacuum-tube solar collector coupled with a LHTES containing 45 kg of erythritol as PCM. The results showed that the system was able to cook twice (noon and evening) in a summer day in Japan.

Kaizawa et al. [191] studied the thermal and flow behaviors in a trans-heat container including 80 kg of erythritol as PCM. The authors concluded that the shape of the inlet pipes should be designed by considering their position, the number of pipes, and the nozzle angle using a complex heat and fluid flow model to maximize the heat storage density and heat exchange rate.

Chen et al. [203] conducted a numerical analysis of different PCMs used as heat storage in solar box cookers. The PCMs selected for this study were magnesium nitrate hexahydrate, stearic acid, acetamide, acetanilide, and erythritol. The results of the numerical model showed that: high thermal conductivity values of the container materials did not significantly affect the melt fraction except for very low thermal conductivities; the thickness of the container did not have a significant effect on the melt fraction; the container wall temperatures were very important during the PCM melting process.

Agyenim et al. [192] designed and experimentally studied a LHTES system based on a horizontal concentric tube heat exchanger that incorporated 20.2 kg of erythritol as PCM. The results proved that the system with longitudinal fins provided the best performance.

Agyenim et al. [193] experimentally analyzed the thermal characteristics of a LHTES consisting of an horizontal shell-and-tube heat exchanger filled with erythritol as PCM. By analyzing isothermal contour plots and temperature-time curves, the authors found that the phase change in the four-tube system was dominated by the convective heat transfer, whereas conductive heat transfer was prevailing in the single-tube configuration.

Agyenim et al. [180] experimentally studied the thermal behavior and heat transfer characteristics of a concentric-annulus LHTES for a $LiBr/H_2O$ solar absorption cooling system. The LHTES unit was filled with 20 kg of erythritol

as PCM and was augmented with longitudinal fins on the shell side. The results showed that more than 70 % of the maximum energy charged in the LHTES was recovered during the solidification of erythritol at an average temperature of 80 °C.

Lecuona et al. [204] evaluated an innovative layout of a portable parabolic trough-type solar concentration cooker equipped with a daily thermal storage utensil. The LHTES unit consists of two cylindrical stainless-steel pots with the PCM inserted into the cavity formed between the two. The authors selected erythritol and paraffin wax as PCMs. The results showed that it was possible to cook three meals for a family in both summer and winter.

Nomura et al. [194, 195] experimentally studied the heat storage performance of a direct-contact latent heat exchanger comprising a vertical cylindrical LHTES unit with erythritol as PCM and heat-transfer oil. In these studies, it was concluded that the direct-contact heat exchanger can rapidly release the latent heat stored in the PCM under specific flow conditions of the heat-transfer oil.

Tarwidi [205] numerically analyzed the thermal performances of different PCMs used in a LHTES unit for solar cookers. The studied PCMs (i.e., erythritol, magnesium nitrate hexahydrate, RT100, and magnesium chloride hexahydrate) were inserted in hollow cylinders which were placed in a larger tank. The results provided by the model showed that magnesium chloride hexahydrate was the PCM with the highest capacity to store solar thermal energy.

Papadimitratos et al. [210] experimentally evaluated the thermal performance of a solar water heater with evacuated tubes integrated with PCMs. Two distinct PCMs, namely tritriacontane and erythritol, were used in the studied system. The results showed that the PCMs integrated in the system can effectively store latent heat and enable a delayed cooling after sunset or late evening.

Unger et al. [206] realized and tested an insulated solar electric cooker equipped with a LHTES based on erythritol as PCM. The final prototype was able to boil 1 liter of water in less than 20 minutes with a device efficiency of 35 % and continued to store energy for more than 4 hours.

Mayilvelnathan and Arasu [162] experimentally investigated the heat transfer characteristics during the charging and discharging processes of 1 wt% graphene nanoparticles dispersed in erythritol in a shell and helical tube storage tank. It was concluded that the PCM composed of graphene nanoparticles dispersed in erythritol has superior heat transfer behavior compared to base erythritol.

Abreha et al. [196] designed and manufactured a shell-and-tube kind of LHTES with multiple finned heat transferring fluid tubes. The system used erythritol as PCM and cooking waste oil as heat transfer fluid (HTF). The authors concluded that the proposed LHTES exhibits a very good heat storage capacity.

Mawire et al. [207] realized two identical solar cooking storage pots which were tested in the presence and absence of solar radiation. One pot was filled with a sensible heat storage (i.e., sunflower oil), while the other was filled with a PCM (i.e., erythritol). The results of the tests in the presence of solar radiation showed that the pot filled with sunflower oil ensured a lower cooking time than that of the pot filled with erythritol.

A portable solar box cooker coupled with a LHTES based on a PCM was constructed and tested by Coccia et al. [74]. The storage system, consisting of two interconnected stainless steel pots, had 2.5 kg of erythritol in its cavity. The results showed that the presence of erythritol stabilized the entire system by considerably extending the cooling time of the silicone oil.

The heat storage and phase change performance of a PCM embedded in a LHTES system was investigated experimentally and numerically by He et al. [197]. The PCM and the HTF were erythritol and Thermia Heat Transfer Oil C, respectively. The experimental results showed that the charging process consisted of 3 stages: the channel formation phase, the fusion phase and the final phase. In the first stage, the heat transfer happened via thermal conduction; in the second stage, instead, the transfer was dominated by convection.

An insulated solar electric cooker contained 2.5 kg of erythritol as PCM and connected to a 100 W photovoltaic module was experimentally analyzed by Osei et al. [208]. The authors pointed out that the thermal conductivity of erythritol

could be improved with the addition of aluminum shavings and foils. Moreover, it was explained that no practical difficulties were due to its supercooling since the crystallization of erythritol could be easily triggered by adding cold food, or by inserting a wire coated with crystallized erythritol film into the PCM.

Anilkumar et al. [209] used several multi-criteria decision-making techniques to select the optimal PCM to be employed in a solar box cooker. Based on the numerical results and the following experimental validation, the authors suggested erythritol as the best PCM to be used in LHTES unit for a solar box cooker.

A mobilized thermal energy storage (M-TES) system for heat distribution using erythritol as PCM was analyzed in various studies [211, 215, 216, 212, 213, 214, 217, 218].Firstly, a direct-contact M-TES system based on erythritol as PCM was built and tested on a laboratory scale by Wang et al. [211]. Its thermal performance was tested using a oil/water tank, an electrical boiler, a oil/water pump, and a plate heat exchanger. The results showed that the problem of supercooling of erythritol was totally solved by the dynamic heat exchange between erythritol and HTF.

In 2013, Li et al. [215] presented an economic evaluation of a conceptual M-TES system. The authors noted that the variation in the cost of supplying 1 kWh of thermal energy by using a M-TES is proportional to the transport distance and inversely proportional to the heat demand. It was showed that the use of erythritol over water is more suitable in the case of larger heat demand or longer transport distance.

Guo et al. [216] focused on enhancing the heat transfer in a M-TES system based on erythritol and shortening its charging time. The results provided by a numerical model showed that the charging time could be reduced by approximately 25 %, 26 %, and 29 % by increasing the flow rate of thermal oil, creating channels before charging, or adding a wall heating, respectively, compared to the charging time experimentally obtained with a thermal oil flow rate of 9.8 l/min.

Wang et al. [212] analyzed the heat charge/discharge performance of direct

and indirect contact M-TES containers with erythritol as PCM. It was shown that the results of the cycling stability analysis do not clearly influence the heat charge/discharge processes of the systems. In fact, the results showed that the heat discharge process of the direct contact M-TES container was much faster than the charging process. It has been found that the increased flow rate of the HTF can effectively improve the charge/discharge processes.

Wang et al. [213] and Wang et al. [214] built a direct-contact M-TES based on erythritol and HTF and carried out an experimental and simulation study to evaluate its heat storage performance. The results showed that the PCM in the middle area of the storage unit melted faster than other parts as the heat transfer was faster on the liquid-solid interface. Instead, the erythritol attached to the storage unit wall melted slowly due to the low conductivity of PCM.

More recently, Guo et al. [218] numerically studied the melting and solidification behaviors of erythritol used as PCM in an indirect contact M-TES container. A numerical model (validated by experimental results) was developed to investigate the effect of the following enhancements: the addition of expanded graphite to pure PCM, adjustment of the diameter of the tube containing the HTF and the internal structure of the container, and the installation of fins around the tubes. Applying all three options simultaneously, they achieved a 74 % reduction in charge time and a 67 % reduction in discharge time.

The heat transfer mechanism in a horizontal shell-and-multi-finned-tube LHTES unit based on erythritol, in which the HTF flowed inside the tubes, was experimentally investigated by Anish et al. [198]. To solve the problem of low thermal conductivity of erythritol, Anish et al. [199] numerically studied the effects of different design parameters regarding tubes and fins on the storage performance.

Anish et al. [200] experimentally analyzed the melting and solidification behavior of erythritol in a double spiral coil LHTES unit. The authors observed an increase in the time required for the PCM to melt as the inlet temperature and flow rate of the HTF decreased. On the other hand, the decrease of the HTF flow rate did not have a significant influence on the solidification process

compared to the melting process.

Anish et al. [201] carried out an experimental comparison of the thermal performance of erythritol and xylitol in a double spiral coil LHTES systems considering different flow rates of the HTF (Therminol-55) and inlet temperatures. At the same temperature variation and mass flow rate, erythritol stored 790 kJ of thermal energy in 60 min for a HTF inlet temperature of 155 °C, while xylitol stored 450 kJ of thermal energy in 35 min. The authors concluded that erythritol showed better charging properties than xylitol; however, the discharge performance of erythritol was negatively affected by supercooling.

5.2. Xylitol

Anish et al. [219] studied the thermal behavior during the melting and solidification processes of xylitol in a vertical double-spiral heat exchanger LHTES system. The low thermal conductivity of xylitol caused significant thermal resistance against heat transfer within the PCM. The authors observed that the xylitol-based TES system was able to store about 450 kJ of thermal energy in 35 min during the charging process (flow rate of 2.5 l/m and inlet temperature of 130 °C) and discharged 345 kJ in 50 min during the discharging process (flow rate of 2.5 l/m and inlet temperature of 45 °C). It is worthwhile pointing out that no comments regarding the very stable supercooling and the resistance to crystallization of xylitol were reported in the works of Anish et al. [201] and Anish et al. [219].

In order to recover the coolant waste heat of a vehicle engine and to reuse it for heating the engine and warming the passenger compartment, Shon et al. [220] designed and experimentally studied a heat exchanger containing xylitol as PCM. The results of the heating tests (conducted under minimum conditions) showed that the heating time was reduced by 33.7 % after the installation of the heat exchanger.

A vertical cylindrical shell and a finned tube LHTES with a sensible heat fluid was used by Saikrishnan et al. [85] to investigate the thermal performance of the charging process of the entire system. The PCM selected for the study

was xylitol, while the sensible heat storage medium used was water. The results showed that during the PCM phase transition, the heat transfer was influenced by the fins located on the tube surface, by the temperature, and by the flow rate of the HTF.

The thermal behavior of xylitol inserted in a LHTES system coupled to a portable solar box cooker was studied through an outdoor experimental campaign by Coccia et al. [73]. Because of the very stable supercooling and the difficulties in crystallization of xylitol, the LHTES system was coupled with a manual mixing device in order to trigger its nucleation. Results showed that the average load cooling time taken by the HTF to go from a temperature of 110 °C to 80 °C increased by approximately 346% when the xylitol in the LHTES was triggered.

5.3. Mannitol

The thermal performance of a high-temperature PCM-based TES system for solar cooling and refrigeration applications were tested on a pilot plant scale by Oró et al. [223]. The authors selected d-mannitol (T_{m} = 167 °C) and hydroquinone (T_{m} = 172.2 °C) as PCMs. The results showed that: the two PCMs did not show any hysteresis; a very low supercooling for the hydroquinone was observed in the pilot plant tests, although it was evident in the DSC analysis; a high supercooling of d-mannitol was observed both in the DSC measurements and during the discharge process in the pilot plant tests.

Gil et al. [224] tested d-mannitol and hydroquinone as PCMs in a LHTES system for solar cooling applications. The experimental results showed no hysteresis in either PCM and an evident supercooling for d-mannitol during the discharging process.

The thermal performance of a mannitol-based latent heat accumulator for a solar water heating system was studied by Ling et al. [221]. The results showed that: 14 kg of fully melted mannitol could heat 100 liters of water from 30 to 50 °C in 6 hours; supercooling could be observed during the release of latent heat; the acceleration of the process was influenced by both the mass flow rate and

the inlet temperature of the thermal oil, but their effect was limited.

Peiró et al. [225] experimentally evaluated the advantages of using several PCMs simultaneously in LHTES systems. The PCMs selected were hydroquinone and d-mannitol while a synthetic oil, Therminol VP1, was chosen as HTF. The results showed that, when the selected PCMs were used simultaneously, the inlet and outlet temperatures of the fluid were more uniform.

Kumaresan et al. [222] evaluated the thermal performance of a new type of cooking unit called "tava type" integrated with a LHTES system based on d-mannitol. The cooking tests carried out by the authors showed that olive oil reached a temperature of 152 °C in 15 minutes; this time is relatively short when compared with that required by a conventional liquefied petroleum gas stove in slow cooking mode to achieve the same condition.

Zhang et al. [113] designed a volumetric solar absorber containing d-mannitol as PCM. Moreover, a low concentration of acetylene black nanoparticles were added to the PCM to achieve a uniform temperature distribution and maintain a high phase change enthalpy of the studied SA. The results showed that the system could reach a temperature at the base of the PCM of 198.2 °C, corresponding to an open circuit voltage of 0.65 V.

5.4. Sorbitol

Beemkumar et al. [226] studied the thermal behavior of an experimental setup developed to study the heat transfer of a cascade LHTES system containing encapsulated spheres with internally welded fins filled with three PCMs (i.e., d-mannitol, d-sorbitol, and paraffin wax). The results showed that the highest energy transfer rate in the charge and discharge processes was achieved by using the copper-encapsulated annular finned spheres filled with d-mannitol.

Beemkumar et al. [227] evaluated the thermal performance of a parabolic trough collector with Therminol-66 as HTF and a LHTES system based on encapsulated d-sorbitol. By comparing the results obtained with the various materials and the cost per kW, it was concluded that brass-encapsulated PCM spheres seemed to be a good option for thermal energy storage using d-sorbitol

as PCM.

6. Conclusions and future outlook

For the first time, this paper presented a literature review of the main thermophysical properties of sugar alcohols (SAs), substances that have the potential to be effective solutions when used as phase change materials (PCMs) in latent heat thermal energy storages (LHTESs). The paper also offers an insight on the thermal stability of SAs, along with a focus on the main engineering applications using sugar alcohols as PCMs of LHTESs. In this review, many advantages and issues of six SAs (erythritol, xylitol, mannitol, inositol, sorbitol, dulcitol) were analyzed and discussed. In general, it is possible to assess that some of the studied SAs could be considered suitable for low-to-medium temperature LHTES applications (80–250 °C), provided that their drawbacks are adequately taken into account. Indeed, as shown by different literature works, their natural derivation, low environmental impact, non-toxicity, non-flammability and abundant availability make them competitive and safe materials. Here, a final summary of the main aspects found in the analysis is reported, with the aim to guide interested readers in the choice and evaluation of SAs, both for purposes of fundamental research and thermal applications.

- Very few experimental data are available for the thermophysical properties of some of the studied SAs (i.e., sorbitol, inositol and dulcitol). Moreover, data for density, viscosity and thermal conductivity are generally scarce. These properties, however, are of great importance to deeply understand the physical behavior of SAs.

- While several thermal stability analyses for erythritol and mannitol are available in the literature, a very limited number or no works reporting these analyses have been found for the other evaluated SAs.

- Comparing the results of the available studies, it is clear that the values of some properties are not consistent. This is especially true for thermal

stability studies.

- All the SAs considered in the present analysis have a high latent heat of fusion (> 200 J/g), with the exception of sorbitol, which has a lower value of ΔH_{m} (< 180 J/g). This could limit its use as PCM in LHTESs.

- The main issues that hinder the use of SAs as PCMs in LHTESs are supercooling, low thermal conductivity and thermal stability. Supercooling degree can be high or low for erythritol, mannitol, inositol and dulcitol, and can be reduced by using passive nucleation triggering techniques (e.g., use of nucleating agents or their micro-encapsulation). On the other hand, xylitol and sorbitol have a very stable supercooling due to their resistance to crystallization, and in this case active nucleation triggering techniques should be taken into account (e.g., air lift reactors, stirring, mechanical and bubble agitation, etc.). Several works available in literature used one or more of such techniques profitably for xylitol.

- Thermal conductivity of SAs is generally low and this affects their charging/discharging times when used in LHTESs. Different techniques can be used to enhance their thermal conductivity, e.g. by using composite materials that include either the absorption of SAs into the pores of a supporting material or the addition of a small amount of materials with high thermal conductivity directly into the SAs.

- In terms of thermal stability, SAs suffer from oxidation when they are exposed to air during heating processes. In this regard, erythritol was found to have the best thermal endurance characteristics, while mannitol is not stable even under inert atmosphere. In addition, dulcitol showed quick and severe degradation of its thermal properties with just a few cycles. Thermal stability issues of SAs may be overcome by using specific methods, e.g. inert protective atmospheres, dispersion of nanoparticles into the SAs, development of PCM composites, use of antioxidants.

- Among all SAs, erythritol is the substance that was studied with greatest

interest. Lots of data are available for both its thermophysical properties and thermal stability. Also, the literature is rich of energy applications that use erythritol as PCM.

- Despite its thermal stability issues, mannitol was evaluated in several LHTES applications. It should be noted that the possibility to use mannitol as PCM in specific applications depends on the required number of storage cycles and on the retention temperature above the melting temperature of these applications. For this reason, some authors pointed out that mannitol should not be considered a proper PCM candidate.

- One of the most interesting applications for SAs includes their use in solar cookers. However, only a very limited number of studies evaluated the long-term thermal performance and stability of SAs in real applications. This is also true for SAs used in solar cookers.

In conclusion, it is important to remark that, while certain features and properties of some SAs are widely studied and analyzed, other aspects should be investigated in more detail to deeply understand their potential and to discover new techniques to reduce their negative aspects. For this reason, additional experimental data for density, viscosity, specific heat, and thermal conductivity are needed, especially for sorbitol, inositol, and dulcitol. Further analyses on the thermal stability of SAs should be carried out to clearly quantify after how many storage cycles the degradation of the material is evident, both in terms of mass loss and deterioration of thermophysical properties. In this regard, it could be crucial to develop standardized procedures for the long-term stability analysis that allow to obtain results which describe the real bulk properties of the tested materials. Additional researches on innovative techniques to solve supercooling issue are necessary: methods to trigger nucleation of the substance should be developed and tested to speed up the crystallization process or to activate it when necessary. Further studies of alternative materials to be added to SAs to increase their thermal conductivity or to improve other properties should be addressed.

Acknowledgments

The authors would like to express their gratitude to the technicians of the Institute of Construction and Building Materials of the Technical University of Darmstadt, Germany, for their availability and assistance with the DSC analysis and TGA measurements of sugar alcohols.

Funding

This research did not receive any specific grant from funding agencies in the public, commercial, or not-for-profit sectors.

Nomenclature

Latin Symbols

c_p	Specific heat (J/(g°C))
CR	Cooling rate (°C/min)
HR	Heating rate (°C/min)
T	Temperature (°C)
$T_\mathrm{onset,i}$	Initial onset temperature (°C)
T_max	Maximum thermal stable temperature (°C)

Greek Symbols

Δ	Delta difference
ΔH	Latent heat (J/g)
λ	Thermal conductivity (W/(m°C))
μ	Dynamic viscosity (Pa s)
ρ	Density (kg/m^3)

Subscripts

c	Crystallization
comp	Composite
deg	Degradation
l	Liquid
m	Melting
s	Solid
SA	Sugar alcohol

Acronyms

DSC	Differential scanning calorimetry
FTIR	Fourier transform infrared spectroscopy
HTF	Heat transfer fluid
LHTES	Latent heat thermal energy storage
M − TES	Mobilized thermal energy storage
NFPA	National Fire Protection Association
PCM	Phase change material
SA	Sugar alcohol
TES	Thermal energy storage
TGA	Thermogravimetric analysis
UV	Ultraviolet

References

[1] G. Alva, L. Liu, X. Huang, G. Fang, Thermal energy storage materials and systems for solar energy applications, Renewable and Sustainable Energy Reviews 68 (2017) 693–706.

[2] I. Sarbu, C. Sebarchievici, A comprehensive review of thermal energy storage, Sustainability 10 (2018) 191.

[3] Y. Tao, Y.-L. He, A review of phase change material and performance enhancement method for latent heat storage system, Renewable and Sustainable Energy Reviews 93 (2018) 245–259.

[4] F. Agyenim, N. Hewitt, P. Eames, M. Smyth, A review of materials, heat transfer and phase change problem formulation for latent heat thermal energy storage systems (lhtess), Renewable and sustainable energy reviews 14 (2010) 615–628.

[5] K. Pielichowska, K. Pielichowski, Phase change materials for thermal energy storage, Progress in materials science 65 (2014) 67–123.

[6] J. P. Da Cunha, P. Eames, Thermal energy storage for low and medium temperature applications using phase change materials–a review, Applied energy 177 (2016) 227–238.

[7] H. Nazir, M. Batool, F. J. B. Osorio, M. Isaza-Ruiz, X. Xu, K. Vignarooban, P. Phelan, A. M. Kannan, et al., Recent developments in phase change materials for energy storage applications: A review, International Journal of Heat and Mass Transfer 129 (2019) 491–523.

[8] E. Oró, A. De Gracia, A. Castell, M. M. Farid, L. F. Cabeza, Review on phase change materials (pcms) for cold thermal energy storage applications, Applied Energy 99 (2012) 513–533.

[9] J. Gasia, M. Martin, A. Solé, C. Barreneche, L. F. Cabeza, Phase change material selection for thermal processes working under partial load operat-

ing conditions in the temperature range between 120 and 200 °C, Applied Sciences 7 (2017) 722.

[10] J. M. Maldonado, M. Fullana-Puig, M. Martín, A. Solé, Á. G. Fernández, A. De Gracia, L. F. Cabeza, Phase change material selection for thermal energy storage at high temperature range between 210 °C and 270 °C, Energies 11 (2018) 861.

[11] B. Nie, A. Palacios, B. Zou, J. Liu, T. Zhang, Y. Li, Review on phase change materials for cold thermal energy storage applications, Renewable and Sustainable Energy Reviews 134 (2020) 110340.

[12] A. M. Khudhair, M. M. Farid, A review on energy conservation in building applications with thermal storage by latent heat using phase change materials, Energy conversion and management 45 (2004) 263–275.

[13] L. F. Cabeza, A. Castell, C. d. Barreneche, A. De Gracia, A. Fernández, Materials used as pcm in thermal energy storage in buildings: A review, Renewable and Sustainable Energy Reviews 15 (2011) 1675–1695.

[14] L. F. Cabeza, A. Inés Fernández, C. Barreneche, S. Ushak, Pcm storage, Handbook of Clean Energy Systems (2015) 1–23.

[15] Y. Li, N. Nord, Q. Xiao, T. Tereshchenko, Building heating applications with phase change material: A comprehensive review, Journal of Energy Storage 31 (2020) 101634.

[16] N. R. Jankowski, F. P. McCluskey, A review of phase change materials for vehicle component thermal buffering, Applied energy 113 (2014) 1525–1561.

[17] J. Jaguemont, N. Omar, P. Van den Bossche, J. Mierlo, Phase-change materials (pcm) for automotive applications: A review, Applied thermal engineering 132 (2018) 308–320.

[18] M. Liu, Y. Sun, F. Bruno, A review of numerical modelling of high-temperature phase change material composites for solar thermal energy storage, Journal of Energy Storage 29 (2020) 101378.

[19] Y. Dutil, D. R. Rousse, N. B. Salah, S. Lassue, L. Zalewski, A review on phase-change materials: Mathematical modeling and simulations, Renewable and sustainable Energy reviews 15 (2011) 112–130.

[20] M. M. Kenisarin, Thermophysical properties of some organic phase change materials for latent heat storage. a review, Solar Energy 107 (2014) 553–575.

[21] A. Solé, L. Miró, C. Barreneche, I. Martorell, L. F. Cabeza, Review of the t-history method to determine thermophysical properties of phase change materials (pcm), Renewable and Sustainable Energy Reviews 26 (2013) 425–436.

[22] E. Günther, S. Hiebler, H. Mehling, R. Redlich, Enthalpy of phase change materials as a function of temperature: required accuracy and suitable measurement methods, International Journal of Thermophysics 30 (2009) 1257–1269.

[23] W. Su, L. Gao, L. Wang, H. Zhi, Calibration of differential scanning calorimeter (dsc) for thermal properties analysis of phase change material, Journal of Thermal Analysis and Calorimetry 143 (2021) 2995–3002.

[24] H. Badenhorst, L. F. Cabeza, Critical analysis of the t-history method: A fundamental approach, Thermochimica Acta 650 (2017) 95–105.

[25] L. Theresa, R. Velraj, et al., Thermophysical characterization and comparison of pcms using dsc and t-history experimental setup, Materials Research Express 6 (2019) 125527.

[26] A. Hasan, S. McCormack, M. Huang, B. Norton, Characterization of phase change materials for thermal control of photovoltaics using differential

scanning calorimetry and temperature history method, Energy Conversion and Management 81 (2014) 322–329.

[27] C. Rathgeber, L. Miró, L. F. Cabeza, S. Hiebler, Measurement of enthalpy curves of phase change materials via dsc and t-history: When are both methods needed to estimate the behaviour of the bulk material in applications?, Thermochimica Acta 596 (2014) 79–88.

[28] D. Gaona, E. Urresta, J. Marínez, G. Guerrón, Medium-temperature phase-change materials thermal characterization by the t-history method and differential scanning calorimetry, Experimental Heat Transfer 30 (2017) 463–474.

[29] X.-F. Shao, S. Yang, C. Wang, Y.-J. Yang, W.-J. Wang, Y. Zeng, L.-W. Fan, Screening of sugar alcohols and their binary eutectic mixtures as phase change materials for low-to-medium temperature thermal energy storage.(ii): Isothermal melting and crystallization behaviors, Energy 180 (2019) 572–583.

[30] G. Ferrer, A. Solé, C. Barreneche, I. Martorell, L. F. Cabeza, Review on the methodology used in thermal stability characterization of phase change materials, Renewable and Sustainable Energy Reviews 50 (2015) 665–685.

[31] M. K. Rathod, J. Banerjee, Thermal stability of phase change materials used in latent heat energy storage systems: A review, Renewable and sustainable energy reviews 18 (2013) 246–258.

[32] X.-F. Shao, S. Yang, C. Wang, W.-J. Wang, Y. Zeng, L.-W. Fan, Screening of sugar alcohols and their binary eutectic mixtures as phase change materials for low-to-medium temperature thermal energy storage.(iii): Thermal endurance, Energy 209 (2020) 118483.

[33] S. A. Memon, Phase change materials integrated in building walls: A state

of the art review, Renewable and sustainable energy reviews 31 (2014) 870–906.

[34] C. Rathgeber, S. Hiebler, R. Bayón, L. F. Cabeza, G. Zsembinszki, G. Englmair, M. Dannemand, G. Diarce, O. Fellmann, R. Ravotti, et al., Experimental devices to investigate the long-term stability of phase change materials under application conditions, Applied Sciences 10 (2020) 7968.

[35] H. Mehling, L. F. Cabeza, Heat and cold storage with PCM, volume 308, Springer, 2008.

[36] Z. Khan, Z. Khan, A. Ghafoor, A review of performance enhancement of pcm based latent heat storage system within the context of materials, thermal stability and compatibility, Energy conversion and management 115 (2016) 132–158.

[37] F. Hassan, F. Jamil, A. Hussain, H. M. Ali, M. M. Janjua, S. Khushnood, M. Farhan, K. Altaf, Z. Said, C. Li, Recent advancements in latent heat phase change materials and their applications for thermal energy storage and buildings: A state of the art review, Sustainable Energy Technologies and Assessments 49 (2022) 101646.

[38] W. Su, J. Darkwa, G. Kokogiannakis, Review of solid–liquid phase change materials and their encapsulation technologies, Renewable and Sustainable Energy Reviews 48 (2015) 373–391.

[39] X. Jin, H. Hu, X. Shi, X. Zhang, Energy asymmetry in melting and solidifying processes of pcm, Energy Conversion and Management 106 (2015) 608–614.

[40] N. Beaupere, U. Soupremanien, L. Zalewski, Nucleation triggering methods in supercooled phase change materials (pcm), a review, Thermochimica Acta 670 (2018) 184–201.

[41] X. Huang, C. Zhu, Y. Lin, G. Fang, Thermal properties and applications of microencapsulated pcm for thermal energy storage: A review, Applied Thermal Engineering 147 (2019) 841–855.

[42] M. Kibria, M. Anisur, M. Mahfuz, R. Saidur, I. Metselaar, A review on thermophysical properties of nanoparticle dispersed phase change materials, Energy Conversion and Management 95 (2015) 69–89.

[43] M. H. Zahir, S. A. Mohamed, R. Saidur, F. A. Al-Sulaiman, Supercooling of phase-change materials and the techniques used to mitigate the phenomenon, Applied Energy 240 (2019) 793–817.

[44] A. Safari, R. Saidur, F. Sulaiman, Y. Xu, J. Dong, A review on supercooling of phase change materials in thermal energy storage systems, Renewable and Sustainable Energy Reviews 70 (2017) 905–919.

[45] L. Yang, J.-n. Huang, F. Zhou, Thermophysical properties and applications of nano-enhanced pcms: An update review, Energy conversion and management 214 (2020) 112876.

[46] S. Ghosh, M. Sudha, A review on polyols: new frontiers for health-based bakery products, International journal of food sciences and nutrition 63 (2012) 372–379.

[47] J. M. DeMan, J. W. Finley, W. J. Hurst, C. Y. Lee, Principles of food chemistry, volume 478, Springer, 1999.

[48] H. Schiweck, A. Bär, R. Vogel, E. Schwarz, M. Kunz, Sugar alcohols, Ullmann's Encyclopedia of Industrial Chemistry (2000).

[49] R. Sharma, P. Ganesan, V. Tyagi, H. Metselaar, S. Sandaran, Developments in organic solid–liquid phase change materials and their applications in thermal energy storage, Energy Conversion and Management 95 (2015) 193–228.

[50] G. Hormansdorfer, Latent heat storage material and use thereof, 1989. US Patent 4,795,580.

[51] G. Barone, G. Della Gatta, D. Ferro, V. Piacente, Enthalpies and entropies of sublimation, vaporization and fusion of nine polyhydric alcohols, Journal of the Chemical Society, Faraday Transactions 86 (1990) 75–79.

[52] R. A. Talja, Y. H. Roos, Phase and state transition effects on dielectric, mechanical, and thermal properties of polyols, Thermochimica Acta 380 (2001) 109–121.

[53] X.-F. Shao, C. Wang, Y.-J. Yang, B. Feng, Z.-Q. Zhu, W.-J. Wang, Y. Zeng, L.-W. Fan, Screening of sugar alcohols and their binary eutectic mixtures as phase change materials for low-to-medium temperature latent heat storage.(i): Non-isothermal melting and crystallization behaviors, Energy 160 (2018) 1078–1090.

[54] H. Zhang, M. Duquesne, A. Godin, S. Niedermaier, E. P. del Barrio, S. V. Nedea, C. C. Rindt, Experimental and in silico characterization of xylitol as seasonal heat storage material, Fluid Phase Equilibria 436 (2017) 55–68.

[55] G. Diarce, I. Gandarias, A. Campos-Celador, A. García-Romero, U. Griesser, Eutectic mixtures of sugar alcohols for thermal energy storage in the 50–90 c temperature range, Solar Energy Materials and Solar Cells 134 (2015) 215–226.

[56] E. P. Del Barrio, R. Cadoret, J. Daranlot, F. Achchaq, New sugar alcohols mixtures for long-term thermal energy storage applications at temperatures between 70 c and 100 c, Solar Energy Materials and Solar Cells 155 (2016) 454–468.

[57] J. M. Maldonado, Á. G. Fernández, L. F. Cabeza, Corrosion assessment of myo-inositol sugar alcohol as a phase change material in storage systems connected to fresnel solar plants, Molecules 24 (2019) 1383.

[58] E. P. del Barrio, A. Godin, M. Duquesne, J. Daranlot, J. Jolly, W. Alshaer, T. Kouadio, A. Sommier, Characterization of different sugar alcohols as phase change materials for thermal energy storage applications, Solar Energy Materials and Solar Cells 159 (2017) 560–569.

[59] X. Shao, S. Yang, C. Chen, L. Fan, Z. Yu, Temperature-dependent rheological behaviors of binary eutectic mixtures of sugar alcohols for latent heat storage: A comparative study with pure sugar alcohols, Journal of Thermal Science 30 (2021) 2002–2014.

[60] T. Nomura, C. Zhu, A. Sagara, N. Okinaka, T. Akiyama, Estimation of thermal endurance of multicomponent sugar alcohols as phase change materials, Applied Thermal Engineering 75 (2015) 481–486.

[61] A. Paul, L. Shi, C. W. Bielawski, A eutectic mixture of galactitol and mannitol as a phase change material for latent heat storage, Energy Conversion and Management 103 (2015) 139–146.

[62] N. F. P. Association, et al., NFPA 704, Standard System for the Identification of the Hazards of Materials for Emergency Response, National Fire Protection Association, 2017.

[63] M. Grembecka, Sugar alcohols—their role in the modern world of sweeteners: a review, European Food Research and Technology 241 (2015) 1–14.

[64] A. Nezzal, L. Aerts, M. Verspaille, G. Henderickx, A. Redl, Polymorphism of sorbitol, Journal of Crystal Growth 311 (2009) 3863–3870.

[65] A. L. Jesus, S. C. Nunes, M. R. Silva, A. M. Beja, J. Redinha, Erythritol: Crystal growth from the melt, International journal of pharmaceutics 388 (2010) 129–135.

[66] C. Barreneche, A. Gil, F. Sheth, A. I. Fernández, L. F. Cabeza, Effect of d-mannitol polymorphism in its thermal energy storage capacity when it is used as pcm, Solar Energy 94 (2013) 344–351.

[67] Y. Li, P. Han, J. Wang, T. Shi, C. You, Production of myo-inositol: Recent advance and prospective, Biotechnology and Applied Biochemistry (2021).

[68] Y. Lu, L. Wang, F. Teng, J. Zhang, M. Hu, Y. Tao, Production of myo-inositol from glucose by a novel trienzymatic cascade of polyphosphate glucokinase, inositol 1-phosphate synthase and inositol monophosphatase, Enzyme and microbial technology 112 (2018) 1–5.

[69] K.-i. Izutsu, C. Yomota, H. Okuda, T. Kawanishi, T. Yamaki, R. Ohdate, Z. Yu, E. Yonemochi, K. Terada, Effects of formulation and process factors on the crystal structure of freeze-dried myo-inositol, Journal of pharmaceutical sciences 103 (2014) 2347–2355.

[70] A. Sarı, A. Biçer, Ö. Lafçı, M. Ceylan, Galactitol hexa stearate and galactitol hexa palmitate as novel solid–liquid phase change materials for thermal energy storage, Solar energy 85 (2011) 2061–2071.

[71] Z. Cheng, B. Xue, Z. Tan, Q. Shi, Low-temperature heat capacity and standard thermodynamic functions of d-galactose and galactitol, Chemical Research in Chinese Universities 31 (2015) 987–991.

[72] S. S. Jagtap, A. A. Bedekar, J.-J. Liu, Y.-S. Jin, C. V. Rao, Production of galactitol from galactose by the oleaginous yeast rhodosporidium toruloides ifo0880, Biotechnology for biofuels 12 (2019) 1–13.

[73] G. Coccia, A. Aquilanti, S. Tomassetti, P. F. Muciaccia, G. Di Nicola, Experimental analysis of nucleation triggering in a thermal energy storage based on xylitol used in a portable solar box cooker, Energies 14 (2021) 5981.

[74] G. Coccia, A. Aquilanti, S. Tomassetti, G. Comodi, G. Di Nicola, Design, realization, and tests of a portable solar box cooker coupled with an erythritol-based pcm thermal energy storage, Solar Energy 201 (2020) 530–540.

[75] A. Seppälä, A. Meriläinen, L. Wikström, P. Kauranen, The effect of additives on the speed of the crystallization front of xylitol with various degrees of supercooling, Experimental thermal and fluid science 34 (2010) 523–527.

[76] M. Delgado, M. Navarro, A. Lázaro, S. A. Boyer, E. Peuvrel-Disdier, Triggering and acceleration of xylitol crystallization by seeding and shearing: Rheo-optical and rheological investigation, Solar Energy Materials and Solar Cells 220 (2021) 110840.

[77] S. Puupponen, V. Mikkola, T. Ala-Nissila, A. Seppälä, Novel microstructured polyol–polystyrene composites for seasonal heat storage, Applied energy 172 (2016) 96–106.

[78] C. Huang, Z. Chen, Y. Gui, C. Shi, G. G. Zhang, L. Yu, Crystal nucleation rates in glass-forming molecular liquids: D-sorbitol, d-arabitol, d-xylitol, and glycerol, The Journal of chemical physics 149 (2018) 054503.

[79] V. Brancato, A. Frazzica, A. Sapienza, A. Freni, Identification and characterization of promising phase change materials for solar cooling applications, Solar Energy Materials and Solar Cells 160 (2017) 225–232.

[80] L. Carpentier, S. Desprez, M. Descamps, Crystallization and glass properties of pentitols, Journal of thermal analysis and calorimetry 73 (2003) 577–586.

[81] A. Kaizawa, N. Maruoka, A. Kawai, H. Kamano, T. Jozuka, T. Senda, T. Akiyama, Thermophysical and heat transfer properties of phase change material candidate for waste heat transportation system, Heat and mass transfer 44 (2008) 763–769.

[82] H. Zhou, L. Lv, Y. Zhang, M. Ji, K. Cen, Preparation and characterization of a shape-stable xylitol/expanded graphite composite phase change material for thermal energy storage, Solar Energy Materials and Solar Cells 230 (2021) 111244.

[83] R. Jia, K. Sun, R. Li, Y. Zhang, W. Wang, H. Yin, D. Fang, Q. Shi, Z. Tan, Heat capacities of some sugar alcohols as phase change materials for thermal energy storage applications, The Journal of Chemical Thermodynamics 115 (2017) 233–248.

[84] S. Höhlein, A. König-Haagen, D. Brüggemann, Thermophysical characterization of mgcl2· 6h2o, xylitol and erythritol as phase change materials (pcm) for latent heat thermal energy storage (lhtes), Materials 10 (2017) 444.

[85] V. Saikrishnan, A. Karthikeyan, B. Selvaraj, Experimental study on thermal performance of xylitol in a latent heat storage combined with sensible heat storage, in: AIP Conference Proceedings, volume 2161, AIP Publishing LLC, 2019, p. 020038.

[86] B. Tong, Z.-C. Tan, Q. Shi, Y.-S. Li, D.-T. Yue, S.-X. Wang, Thermodynamic investigation of several natural polyols (i): Heat capacities and thermodynamic properties of xylitol, Thermochimica acta 457 (2007) 20–26.

[87] V. Saikrishnan, A. Karthikeyan, A. Laksmisankar, N. Beemkumar, Thermophysical characteristic analysis of edible erythritol and xylitol for their use as phase change materials, Int. J. Sci. Tech 8 (2019) 644–649.

[88] H. P. Diogo, S. S. Pinto, J. J. M. Ramos, Slow molecular mobility in the crystalline and amorphous solid states of pentitols: a study by thermally stimulated depolarisation currents and by differential scanning calorimetry, Carbohydrate research 342 (2007) 961–969.

[89] H. Cammenga, I. Steppuhn, Polymorphic status of sorbitol: solution calorimetry versus dsc, Thermochimica acta 229 (1993) 253–256.

[90] Á. Gombás, P. Szabó-Révész, G. Regdon, I. Erős, Study of thermal behaviour of sugar alcohols, Journal of thermal analysis and calorimetry 73 (2003) 615–621.

[91] D. N. Bolmatenkov, M. I. Yagofarov, A. A. Sokolov, M. A. Ziganshin, B. N. Solomonov, The heat capacities and fusion thermochemistry of sugar alcohols between 298.15 k and tm: The study of d-sorbitol, d-mannitol and myo-inositol, Journal of Molecular Liquids 330 (2021) 115545.

[92] B. Tong, Z. Tan, Q. Shi, Y. Li, S. Wang, Thermodynamic investigation of several natural polyols (ii) heat capacities and thermodynamic properties of sorbitol, Journal of thermal analysis and calorimetry 91 (2008) 463–469.

[93] B. Jeganathan, V. Prakya, Design and optimization of novel sugar alcohol based extended release tablets prepared by melt dispersion technique, Iranian Journal of Pharmaceutical Sciences 8 (2012) 83–98.

[94] K. Bitchikh, A. Meniai, W. Louaer, Measurement and prediction of binary and ternary liquid-solid equilibria of pharmaceutical and food systems, Energy Procedia 18 (2012) 1152–1164.

[95] H. Che, Q. Chen, Q. Zhong, S. He, The effects of nanoparticles on morphology and thermal properties of erythritol/polyvinyl alcohol phase change composite fibers, e-Polymers 18 (2018) 321–329.

[96] B. Yang, N. Wang, Y. Song, J. Liu, Study on the improvement of supercooling and thermal properties of erythritol-based phase change energy storage materials, Renewable Energy 175 (2021) 80–97.

[97] M. Vivekananthan, V. A. Amirtham, Characterisation and thermophysical properties of graphene nanoparticles dispersed erythritol pcm for medium temperature thermal energy storage applications, Thermochimica Acta 676 (2019) 94–103.

[98] H. Zhang, J. Cheng, Q. Wang, D. Xiong, J. Song, Z. Tang, X. Liu, The graphite foam/erythritol composites with ultrahigh thermal conductivity for medium temperature applications, Solar Energy Materials and Solar Cells 230 (2021) 111135.

[99] J.-L. Zeng, L. Zhou, Y.-F. Zhang, S.-L. Sun, Y.-H. Chen, L. Shu, L.-P. Yu, L. Zhu, L.-B. Song, Z. Cao, Effects of some nucleating agents on the supercooling of erythritol to be applied as phase change material, Journal of Thermal Analysis and Calorimetry 129 (2017) 1291–1299.

[100] Y. Wang, S. Li, T. Zhang, D. Zhang, H. Ji, Supercooling suppression and thermal behavior improvement of erythritol as phase change material for thermal energy storage, Solar Energy Materials and Solar Cells 171 (2017) 60–71.

[101] N. Tan, T. Xie, Y. Feng, P. Hu, Q. Li, L.-M. Jiang, W.-B. Zeng, J.-L. Zeng, Preparation and characterization of erythritol/sepiolite/exfoliated graphite nanoplatelets form-stable phase change material with high thermal conductivity and suppressed supercooling, Solar Energy Materials and Solar Cells 217 (2020) 110726.

[102] Y.-H. Chen, L.-M. Jiang, Y. Fang, L. Shu, Y.-X. Zhang, T. Xie, K.-Y. Li, N. Tan, L. Zhu, Z. Cao, et al., Preparation and thermal energy storage properties of erythritol/polyaniline form-stable phase change material, Solar Energy Materials and Solar Cells 200 (2019) 109989.

[103] M. Yuan, C. Xu, T. Wang, T. Zhang, X. Pan, F. Ye, Supercooling suppression and crystallization behaviour of erythritol/expanded graphite as form-stable phase change material, Chemical Engineering Journal 413 (2021) 127394.

[104] S. Bao, Q. Wei, J. Cao, H. Li, L. Ma, J. An, C.-T. Lin, J. Luo, K. Zhou, Hydrophilic modification of carbon nanotube to prepare a novel porous copper network-carbon nanotube/erythritol composite phase change material, Composite Interfaces 28 (2021) 175–189.

[105] A. Shobo, A. Mawire, Experimental comparison of the thermal performances of acetanilide, meso-erythritol and an in-sn alloy in similar spherical capsules, Applied Thermal Engineering 124 (2017) 871–882.

[106] A. Sari, R. Eroglu, A. Bicer, A. Karaipekli, Synthesis and thermal energy storage properties of erythritol tetrastearate and erythritol tetrapalmitate, Chemical engineering & technology 34 (2011) 87–92.

[107] Y. Wang, Z. Zhang, T. Zhang, Z. Qin, D. Zhang, H. Ji, Preparation and characterization of erythritol/graphene oxide shape-stable composites with improved thermal-physical property, ChemistrySelect 4 (2019) 1149–1157.

[108] A. Solé, H. Neumann, S. Niedermaier, L. F. Cabeza, E. Palomo, Thermal stability test of sugar alcohols as phase change materials for medium temperature energy storage application, Energy Procedia 48 (2014) 436–439.

[109] A. Sari, Thermal energy storage properties of mannitol–fatty acid esters as novel organic solid–liquid phase change materials, Energy conversion and management 64 (2012) 68–78.

[110] S. Salyan, B. Praveen, H. Singh, S. Suresh, A. S. Reddy, Liquid metal gallium in metal inserts for solar thermal energy storage: A novel heat transfer enhancement technique, Solar Energy Materials and Solar Cells 208 (2020) 110365.

[111] V. Pethurajan, S. Sivan, A. J. Konatt, A. S. Reddy, Facile approach to improve solar thermal energy storage efficiency using encapsulated sugar alcohol based phase change material, Solar Energy Materials and Solar Cells 185 (2018) 524–535.

[112] L. He, S. Mo, P. Lin, L. Jia, Y. Chen, Z. Cheng, Synthesis and properties of nanoencapsulated d-mannitol for medium temperature thermal energy storage, Solar Energy Materials and Solar Cells 209 (2020) 110473.

[113] X. Zhang, Z. Du, Y. Zhu, C. Li, X. Hu, T. Yang, B.-B. Yu, R. Gu, Y. Ding, Z. He, A novel volumetric absorber integrated with low-cost d-mannitol and acetylene-black nanoparticles for solar-thermal-electricity generation, Solar Energy Materials and Solar Cells 207 (2020) 110366.

[114] R. Bayón, E. Rojas, Characterization of organic pcms for medium temperature storage, Materials and Technologies for Energy Efficiency, Brown Walker Press, Boca Ratón, Florida (US) (2015) 157–161.

[115] H. Liu, Z. Qian, Q. Wang, D. Wu, X. Wang, Development of renewable biomass-derived carbonaceous aerogel/mannitol phase-change composites for high thermal-energy-release efficiency and shape stabilization, ACS Applied Energy Materials 4 (2021) 1714–1730.

[116] D. Singh, S. Suresh, H. Singh, Graphene nanoplatelets enhanced myo-inositol for solar thermal energy storage, Thermal Science and Engineering Progress 2 (2017) 1–7.

[117] R. T. Alarcon, C. Gaglieri, F. J. Caires, A. G. Magdalena, R. A. E. de Castro, G. Bannach, Thermoanalytical study of sweetener myo-inositol: α and β polymorphs, Food chemistry 237 (2017) 1149–1154.

[118] S. Mo, Y. Li, S. Shan, L. Jia, Y. Chen, Synthesis and properties of inositol nanocapsules, Materials 14 (2021) 5481.

[119] K. Nakano, Y. Masuda, H. Daiguji, Crystallization and melting behavior of erythritol in and around two-dimensional hexagonal mesoporous silica, The Journal of Physical Chemistry C 119 (2015) 4769–4777.

[120] M. Duquesne, E. Palomo Del Barrio, A. Godin, Nucleation triggering of highly undercooled xylitol using an air lift reactor for seasonal thermal energy storage, Applied Sciences 9 (2019) 267.

[121] L. Piquard, E. Gagnière, G. Largiller, D. Mangin, F. Bentivoglio, Xylitol used as phase change material: Nucleation mechanisms of the supercooling rupture by stirring, Journal of Energy Storage 48 (2022) 103922.

[122] A. Godin, M. Duquesne, E. P. del Barrio, F. Achchaq, P. Monneyron, Bubble agitation as a new low-intrusive method to crystallize glass-forming materials, Energy Procedia 139 (2017) 352–357.

[123] E. P. Ona, X. Zhang, S. Ozawa, H. Matsuda, H. Kakiuchi, M. Yabe, M. Yamazaki, M. Sato, Influence of ultrasonic irradiation on the solidification behavior of erythritol as a pcm, Journal of chemical engineering of Japan 35 (2002) 290–298.

[124] J. M. Marín, B. Zalba, L. F. Cabeza, H. Mehling, Improvement of a thermal energy storage using plates with paraffin–graphite composite, International Journal of Heat and Mass Transfer 48 (2005) 2561–2570.

[125] E. P. Ona, X. Zhang, K. Kyaw, F. Watanabe, H. Matsuda, H. Kakiuchi, M. Yabe, S. Chihara, Relaxation of supercooling of erythritol for latent heat storage, Journal of chemical engineering of Japan 34 (2001) 376–382.

[126] S. Yang, X.-F. Shao, L.-W. Fan, Suppressing the supercooling effect of erythritol by bubbling for latent heat storage, in: Heat Transfer Summer Conference, volume 83709, American Society of Mechanical Engineers, 2020, p. V001T11A013.

[127] N. R. Jankowski, F. P. McCluskey, Electrical supercooling mitigation in erythritol, in: International Heat Transfer Conference, volume 49422, 2010, pp. 409–416.

[128] L. Klimeš, P. Charvát, M. M. Joybari, M. Zálešák, F. Haghighat, K. Panchabikesan, M. El Mankibi, Y. Yuan, Computer modelling and experimental investigation of phase change hysteresis of pcms: The state-of-the-art review, Applied Energy 263 (2020) 114572.

[129] S. N. Gunasekara, R. Pan, J. N. Chiu, V. Martin, Polyols as phase change materials for surplus thermal energy storage, Applied Energy 162 (2016) 1439–1452.

[130] S. N. Gunasekara, J. N. Chiu, V. Martin, P. Hedström, The experimental phase diagram study of the binary polyols system erythritol-xylitol, Solar Energy Materials and Solar Cells 174 (2018) 248–262.

[131] Z. Huang, N. Xie, Z. Luo, X. Gao, X. Fang, Y. Fang, Z. Zhang, Characterization of medium-temperature phase change materials for solar thermal energy storage using temperature history method, Solar Energy Materials and Solar Cells 179 (2018) 152–160.

[132] G. S. Parks, C. T. Anderson, Thermal data on organic compounds. iii. the heat capacities, entropies and free energies of tertiary butyl alcohol, mannitol, erythritol and normal butyric acid, Journal of the American Chemical Society 48 (1926) 1506–1512.

[133] Y. Lian, A. Chen, J. Suurkuusk, I. Wadso, Polyol—-water interactions as reflected by aqueous heat capacity values, Acta Chem. Scand. A 36 (1982).

[134] H. Zhang, R. M. van Wissen, S. V. Nedea, C. C. Rindt, Characterization of sugar alcohols as seasonal heat storage media-experimental and theoretical investigations, Proceedings of Advances in Thermal Energy Storage, EUROTHERM 99 (2014).

[135] B. Tong, Z. Tan, J. Zhang, S. Wang, Thermodynamic investigation of several natural polyols, Journal of thermal analysis and calorimetry 95 (2009) 469–475.

[136] L. Zhichao, Z. Qiang, W. Gaohui, Preparation and enhanced heat capacity of nano-titania doped erythritol as phase change material, International Journal of Heat and Mass Transfer 80 (2015) 653–659.

[137] M. E. Spaght, S. B. Thomas, G. S. Parks, Some heat-capacity data on organic compounds obtained with a radiation calorimeter, The Journal of Physical Chemistry 36 (2002) 882–888.

[138] M. Karthik, A. Faik, P. Blanco-Rodríguez, J. Rodríguez-Aseguinolaza, B. D'Aguanno, Preparation of erythritol–graphite foam phase change composite with enhanced thermal conductivity for thermal energy storage applications, Carbon 94 (2015) 266–276.

[139] A. Lopes Jesus, L. I. Tomé, M. E. Eusebio, J. Redinha, Enthalpy of sublimation in the study of the solid state of organic compounds. application to erythritol and threitol, The Journal of Physical Chemistry B 109 (2005) 18055–18060.

[140] I. Kholmanov, J. Kim, E. Ou, R. S. Ruoff, L. Shi, Continuous carbon nanotube–ultrathin graphite hybrid foams for increased thermal conductivity and suppressed subcooling in composite phase change materials, ACS nano 9 (2015) 11699–11707.

[141] B. Tong, R.-B. Liu, C.-G. Meng, F.-Y. Yu, S.-H. Ji, Z.-C. Tan, Heat capacities and nonisothermal thermal decomposition reaction kinetics of d-mannitol, Journal of Chemical & Engineering Data 55 (2010) 119–124.

[142] A. Mojiri, N. Grbac, B. Bourke, G. Rosengarten, D-mannitol for medium temperature thermal energy storage, Solar Energy Materials and Solar Cells 176 (2018) 150–156.

[143] W. F. Magie, The specific heat of solutions. iv, Physical Review (Series I) 17 (1903) 105.

[144] A. Knyazev, V. Emel'yanenko, A. Shipilova, D. Zaitsau, M. Lelet, S. Knyazeva, E. Gusarova, M. Varfolomeev, Thermodynamic properties of myo-inositol, The Journal of Chemical Thermodynamics 116 (2018) 76–84.

[145] F. S. Costa, M. E. Eusébio, J. Redinha, M. L. P. Leitão, Enthalpies of solvation of hydroxyl cyclohexane derivatives in different solvents, The Journal of Chemical Thermodynamics 31 (1999) 895–903.

[146] S. N. Gunasekara, M. Ignatowicz, J. N. Chiu, V. Martin, Thermal conductivity measurement of erythritol, xylitol, and their blends for phase change material design: A methodological study, International Journal of Energy Research 43 (2019) 1785–1801.

[147] Y. Wang, L. Wang, N. Xie, X. Lin, H. Chen, Experimental study on the melting and solidification behavior of erythritol in a vertical shell-and-tube latent heat thermal storage unit, International Journal of Heat and Mass Transfer 99 (2016) 770–781.

[148] M. Yuan, Y. Ren, C. Xu, F. Ye, X. Du, Characterization and stability study of a form-stable erythritol/expanded graphite composite phase change material for thermal energy storage, Renewable energy 136 (2019) 211–222.

[149] L. Gao, J. Zhao, Q. An, D. Zhao, F. Meng, X. Liu, Experiments on thermal performance of erythritol/expanded graphite in a direct contact thermal energy storage container, Applied Thermal Engineering 113 (2017) 858–866.

[150] T. Oya, T. Nomura, M. Tsubota, N. Okinaka, T. Akiyama, Thermal conductivity enhancement of erythritol as pcm by using graphite and nickel particles, Applied Thermal Engineering 61 (2013) 825–828.

[151] Q. Zhang, Z. Luo, Q. Guo, G. Wu, Preparation and thermal properties of short carbon fibers/erythritol phase change materials, Energy conversion and management 136 (2017) 220–228.

[152] C. Ma, J. Wang, Y. Wu, Y. Wang, Z. Ji, S. Xie, Characterization and thermophysical properties of erythritol/expanded graphite as phase change material for thermal energy storage, Journal of Energy Storage 46 (2022) 103864.

[153] S. Salyan, S. Suresh, Study of thermo-physical properties and cycling stability of d-mannitol-copper oxide nanocomposites as phase change materials, Journal of Energy Storage 15 (2018) 245–255.

[154] X. Liu, C. Marbut, D. Huitink, G. Feng, A. S. Fleischer, Influence of crystalline polymorphism on the phase change properties of sorbitol-au nanocomposites, Materials Today Energy 12 (2019) 379–388.

[155] L. Fan, J. M. Khodadadi, Thermal conductivity enhancement of phase change materials for thermal energy storage: a review, Renewable and sustainable energy reviews 15 (2011) 24–46.

[156] S. Wu, T. Yan, Z. Kuai, W. Pan, Thermal conductivity enhancement on phase change materials for thermal energy storage: A review, Energy Storage Materials 25 (2020) 251–295.

[157] V. Tyagi, K. Chopra, R. Sharma, A. Pandey, S. Tyagi, M. S. Ahmad, A. Sarı, R. Kothari, A comprehensive review on phase change materials for heat storage applications: Development, characterization, thermal and chemical stability, Solar Energy Materials and Solar Cells 234 (2022) 111392.

[158] X. Li, J. Zhang, B. Fu, C. Song, W. Shang, P. Tao, T. Deng, Erythritol impregnated within surface-roughened hydrophilic metal foam for medium-temperature solar-thermal energy harvesting, Energy Conversion and Management 222 (2020) 113241.

[159] C. S. Heu, S. W. Kim, K.-S. Lee, D. R. Kim, Fabrication of three-dimensional metal-graphene network phase change composite for high thermal conductivity and suppressed subcooling phenomena, Energy Conversion and Management 149 (2017) 608–615.

[160] R. P. Singh, S. Kaushik, D. Rakshit, Melting phenomenon in a finned thermal storage system with graphene nano-plates for medium temperature applications, Energy Conversion and Management 163 (2018) 86–99.

[161] T. Oya, T. Nomura, N. Okinaka, T. Akiyama, Phase change composite based on porous nickel and erythritol, Applied Thermal Engineering 40 (2012) 373–377.

[162] V. Mayilvelnathan, A. V. Arasu, Experimental investigation on thermal behavior of graphene dispersed erythritol pcm in a shell and helical tube

latent energy storage system, International Journal of Thermal Sciences 155 (2020) 106446.

[163] T. Xu, Q. Chen, G. Huang, Z. Zhang, X. Gao, S. Lu, Preparation and thermal energy storage properties of d-mannitol/expanded graphite composite phase change material, Solar Energy Materials and Solar Cells 155 (2016) 141–146.

[164] X.-F. Shao, C.-L. Chen, Y.-J. Yang, X.-K. Ku, L.-W. Fan, Rheological behaviors of sugar alcohols for low-to-medium temperature latent heat storage: Effects of temperature in both the molten and supercooled liquid states, Solar Energy Materials and Solar Cells 195 (2019) 142–154.

[165] M. P. Alferez Luna, H. Neumann, S. Gschwander, Stability study of erythritol as phase change material for medium temperature thermal applications, Applied Sciences 11 (2021) 5448.

[166] A. Solé, H. Neumann, S. Niedermaier, I. Martorell, P. Schossig, L. F. Cabeza, Stability of sugar alcohols as pcm for thermal energy storage, Solar energy materials and solar cells 126 (2014) 125–134.

[167] A. Burger, J.-O. Henck, S. Hetz, J. M. Rollinger, A. A. Weissnicht, H. Stöttner, Energy/temperature diagram and compression behavior of the polymorphs of d-mannitol, Journal of pharmaceutical sciences 89 (2000) 457–468.

[168] A. Sagara, T. Nomura, M. Tsubota, N. Okinaka, T. Akiyama, Improvement in thermal endurance of d-mannitol as phase-change material by impregnation into nanosized pores, Materials Chemistry and Physics 146 (2014) 253–260.

[169] M.-M. Rodríguez-García, R. Bayón, E. Rojas, Stability of d-mannitol upon melting/freezing cycles under controlled inert atmosphere, Energy Procedia 91 (2016) 218–225.

[170] R. Bayón, E. Rojas, Feasibility study of d-mannitol as phase change material for thermal storage, AIMS Energy 5 (2017) 404–424.

[171] H. Neumann, D. Burger, Y. Taftanazi, M. A. Luna, T. Haussmann, G. Hagelstein, S. Gschwander, Thermal stability enhancement of d-mannitol for latent heat storage applications, Solar Energy Materials and Solar Cells 200 (2019) 109913.

[172] ISO11358-1, Plastics–thermogravimetry (tg) of polymers–part 1: General principles, 2014.

[173] S. Salyan, S. Suresh, Liquid metal gallium laden organic phase change material for energy storage: an experimental study, International Journal of Hydrogen Energy 43 (2018) 2469–2483.

[174] G. John, A. König-Haagen, C. K. King'ondu, D. Brüggemann, L. Nkhonjera, Galactitol as phase change material for latent heat storage of solar cookers: Investigating thermal behavior in bulk cycling, Solar Energy 119 (2015) 415–421.

[175] S. Salyan, S. Suresh, Multi-walled carbon nanotube laden with d-mannitol as phase change material: characterization and experimental investigation, Advanced Powder Technology 29 (2018) 3183–3191.

[176] J.-L. Zeng, Y.-H. Chen, L. Shu, L.-P. Yu, L. Zhu, L.-B. Song, Z. Cao, L.-X. Sun, Preparation and thermal properties of exfoliated graphite/erythritol/mannitol eutectic composite as form-stable phase change material for thermal energy storage, Solar Energy Materials and Solar Cells 178 (2018) 84–90.

[177] L.-M. Jiang, Y.-H. Chen, L. Shu, Y.-X. Zhang, T. Xie, N. Tan, Y. Fang, S.-F. Wang, L. Zhang, J.-L. Zeng, Preparation and characterization of erythritol/polyaniline form-stable phase change materials containing silver nanowires, International Journal of Energy Research 43 (2019) 8385–8397.

[178] M. A. G. Lazcano, W. Yu, Thermal performance and flammability of phase change material for medium and elevated temperatures for textile application, Journal of Thermal Analysis and Calorimetry 117 (2014) 9–17.

[179] G. Kumaresan, R. Velraj, S. Iniyan, Thermal analysis of d-mannitol for use as phase change material for latent heat storage, Journal of applied sciences 11 (2011) 3044–3048.

[180] F. Agyenim, P. Eames, M. Smyth, Experimental study on the melting and solidification behaviour of a medium temperature phase change storage material (erythritol) system augmented with fins to power a libr/h2o absorption cooling system, Renewable energy 36 (2011) 108–117.

[181] A. Shobo, A. Mawire, M. Aucamp, Rapid thermal cycling of three phase change materials (pcms) for cooking applications, Journal of the Brazilian Society of Mechanical Sciences and Engineering 40 (2018) 1–12.

[182] A. Shukla, D. Buddhi, R. Sawhney, Thermal cycling test of few selected inorganic and organic phase change materials, Renewable energy 33 (2008) 2606–2614.

[183] N. Stathopoulos, G. Belessiotis, P. Oikonomou, E. Papanicolaou, Experimental investigation of thermal degradation of phase change materials for medium-temperature thermal energy storage and tightness during cycling inside metal spheres, Journal of Energy Storage 31 (2020) 101618.

[184] D. Singh, S. Suresh, H. Singh, B. Rose, S. Tassou, N. Anantharaman, Myo-inositol based nano-pcm for solar thermal energy storage, Applied Thermal Engineering 110 (2017) 564–572.

[185] H. K. Shin, K.-Y. Rhee, S.-J. Park, Effects of exfoliated graphite on the thermal properties of erythritol-based composites used as phase-change materials, Composites Part B: Engineering 96 (2016) 350–353.

[186] S.-Y. Lee, H. K. Shin, M. Park, K. Y. Rhee, S.-J. Park, Thermal characterization of erythritol/expanded graphite composites for high thermal storage capacity, Carbon 68 (2014) 67–72.

[187] X. Zhang, X. Chen, Z. Han, W. Xu, Study on phase change interface for erythritol with nano-copper in spherical container during heat transport, International Journal of Heat and Mass Transfer 92 (2016) 490–496.

[188] M. Yuan, F. Ye, C. Xu, Supercooling study of erythritol/eg composite phase change materials, Energy Procedia 158 (2019) 4629–4634.

[189] L. Miró, C. Barreneche, G. Ferrer, A. Solé, I. Martorell, L. F. Cabeza, Health hazard, cycling and thermal stability as key parameters when selecting a suitable phase change material (pcm), Thermochimica acta 627 (2016) 39–47.

[190] H. Neumann, S. Niedermaier, S. Gschwander, P. Schossig, Cycling stability of d-mannitol when used as phase change material for thermal storage applications, Thermochimica Acta 660 (2018) 134–143.

[191] A. Kaizawa, H. Kamano, A. Kawai, T. Jozuka, T. Senda, N. Maruoka, T. Akiyama, Thermal and flow behaviors in heat transportation container using phase change material, Energy Conversion and Management 49 (2008) 698–706.

[192] F. Agyenim, P. Eames, M. Smyth, A comparison of heat transfer enhancement in a medium temperature thermal energy storage heat exchanger using fins, Solar Energy 83 (2009) 1509–1520.

[193] F. Agyenim, P. Eames, M. Smyth, Heat transfer enhancement in medium temperature thermal energy storage system using a multitube heat transfer array, Renewable energy 35 (2010) 198–207.

[194] T. Nomura, M. Tsubota, T. Oya, N. Okinaka, T. Akiyama, Heat release performance of direct-contact heat exchanger with erythritol as phase change material, Applied thermal engineering 61 (2013) 28–35.

[195] T. Nomura, M. Tsubota, A. Sagara, N. Okinaka, T. Akiyama, Performance analysis of heat storage of direct-contact heat exchanger with phase-change material, Applied thermal engineering 58 (2013) 108–113.

[196] B. G. Abreha, P. Mahanta, G. Trivedi, Performance investigation of lab-scale shell and tube lhs prototype, Journal of Energy Storage 31 (2020) 101527.

[197] S. He, W. Wang, L. Wei, J. Ding, Heat transfer enhancement and melting behavior of phase change material in a direct-contact thermal energy storage container, Journal of Energy Storage 31 (2020) 101665.

[198] R. Anish, V. Mariappan, S. Suresh, Experimental investigation on melting and solidification behaviour of erythritol in a vertical double spiral coil thermal energy storage system, Sustainable Cities and Society 44 (2019) 253–264.

[199] R. Anish, M. M. Joybari, S. Seddegh, V. Mariappan, F. Haghighat, Y. Yuan, Sensitivity analysis of design parameters for erythritol melting in a horizontal shell and multi-finned tube system: Numerical investigation, Renewable Energy 163 (2021) 423–436.

[200] R. Anish, V. Mariappan, M. M. Joybari, Experimental investigation on the melting and solidification behavior of erythritol in a horizontal shell and multi-finned tube latent heat storage unit, Applied Thermal Engineering 161 (2019) 114194.

[201] R. Anish, V. Mariappan, M. M. Joybari, A. M. Abdulateef, Performance comparison of the thermal behavior of xylitol and erythritol in a double spiral coil latent heat storage system, Thermal Science and Engineering Progress 15 (2020) 100441.

[202] S. Sharma, T. Iwata, H. Kitano, K. Sagara, Thermal performance of a solar cooker based on an evacuated tube solar collector with a pcm storage unit, Solar Energy 78 (2005) 416–426.

[203] C. Chen, A. Sharma, S. Tyagi, D. Buddhi, Numerical heat transfer studies of pcms used in a box-type solar cooker, Renewable Energy 33 (2008) 1121–1129.

[204] A. Lecuona, J.-I. Nogueira, R. Ventas, M. Legrand, et al., Solar cooker of the portable parabolic type incorporating heat storage based on pcm, Applied energy 111 (2013) 1136–1146.

[205] D. Tarwidi, Modeling and numerical simulation of solar cooker with pcm as thermal energy storage, in: 2015 3rd International Conference on Information and Communication Technology (ICoICT), IEEE, 2015, pp. 584–589.

[206] J. B. Unger, N. R. Christler, M. Weeman, M. E. Strutz, Insulated solar electric cooker with phase change thermal storage medium (2019).

[207] A. Mawire, K. Lentswe, P. Owusu, A. Shobo, J. Darkwa, J. Calautit, M. Worall, Performance comparison of two solar cooking storage pots combined with wonderbag slow cookers for off-sunshine cooking, Solar Energy 208 (2020) 1166–1180.

[208] M. Osei, O. Staveland, S. McGowan, J. B. Unger, N. R. Christler, M. Weeman, M. E. Strutz, M. Walker, M. B. Maun, N. C. Dunning, et al., Phase change thermal storage: Cooking with more power and versatility, Solar Energy 220 (2021) 1065–1073.

[209] B. Anilkumar, R. Maniyeri, S. Anish, Optimum selection of phase change material for solar box cooker integrated with thermal energy storage unit using multi-criteria decision-making technique, Journal of Energy Storage 40 (2021) 102807.

[210] A. Papadimitratos, S. Sobhansarbandi, V. Pozdin, A. Zakhidov, F. Hassanipour, Evacuated tube solar collectors integrated with phase change materials, Solar Energy 129 (2016) 10–19.

[211] W. Wang, J. Yan, E. Dahlquist, Thermal performance of the mobilized thermal energy storage system, in: International Conference on Applied Energy, MAY 16-18, 2011 PERUGIA, ITALY, 2011.

[212] W. Wang, S. Guo, H. Li, J. Yan, J. Zhao, X. Li, J. Ding, Experimental study on the direct/indirect contact energy storage container in mobilized thermal energy system (m-tes), Applied energy 119 (2014) 181–189.

[213] W. Wang, S. He, S. Guo, J. Yan, J. Ding, A combined experimental and simulation study on charging process of erythritol–hto direct-blending based energy storage system, Energy conversion and management 83 (2014) 306–313.

[214] W. Wang, H. Li, S. Guo, S. He, J. Ding, J. Yan, J. Yang, Numerical simulation study on discharging process of the direct-contact phase change energy storage system, Applied Energy 150 (2015) 61–68.

[215] H. Li, W. Wang, J. Yan, E. Dahlquist, Economic assessment of the mobilized thermal energy storage (m-tes) system for distributed heat supply, Applied energy 104 (2013) 178–186.

[216] S. Guo, H. Li, J. Zhao, X. Li, J. Yan, Numerical simulation study on optimizing charging process of the direct contact mobilized thermal energy storage, Applied energy 112 (2013) 1416–1423.

[217] S. Guo, J. Zhao, W. Wang, G. Jin, X. Wang, Q. An, W. Gao, Experimental study on solving the blocking for the direct contact mobilized thermal energy storage container, Applied Thermal Engineering 78 (2015) 556–564.

[218] S. Guo, J. Zhao, W. Wang, J. Yan, G. Jin, Z. Zhang, J. Gu, Y. Niu, Numerical study of the improvement of an indirect contact mobilized thermal energy storage container, Applied Energy 161 (2016) 476–486.

[219] R. Anish, V. Mariappan, S. Suresh, M. M. Joybari, A. M. Abdulateef, Experimental investigation on the energy storage/discharge performance

of xylitol in a compact spiral coil heat exchanger, International Journal of Thermal Sciences 159 (2021) 106633.

[220] J. Shon, H. Kim, K. Lee, Improved heat storage rate for an automobile coolant waste heat recovery system using phase-change material in a fin–tube heat exchanger, Applied energy 113 (2014) 680–689.

[221] Z. Ling, G. Zeng, T. Xu, X. Fang, Z. Zhang, Performance of a coil-pipe heat exchanger filled with mannitol for solar water heating system, Energy Procedia 75 (2015) 827–833.

[222] G. Kumaresan, V. Vigneswaran, S. Esakkimuthu, R. Velraj, Performance assessment of a solar domestic cooking unit integrated with thermal energy storage system, Journal of energy storage 6 (2016) 70–79.

[223] E. Oró, A. Gil, L. Miró, G. Peiró, S. Álvarez, L. F. Cabeza, Thermal energy storage implementation using phase change materials for solar cooling and refrigeration applications, Energy Procedia 30 (2012) 947–956.

[224] A. Gil, E. Oró, G. Peiró, S. Álvarez, L. F. Cabeza, Material selection and testing for thermal energy storage in solar cooling, Renewable Energy 57 (2013) 366–371.

[225] G. Peiró, J. Gasia, L. Miró, L. F. Cabeza, Experimental evaluation at pilot plant scale of multiple pcms (cascaded) vs. single pcm configuration for thermal energy storage, Renewable Energy 83 (2015) 729–736.

[226] N. Beemkumar, A. Karthikeyan, D. Yuvarajan, S. L. Sankar, Experimental investigation on improving the heat transfer of cascaded thermal storage system using different fins, Arabian Journal for Science and Engineering 42 (2017) 2055–2065.

[227] N. Beemkumar, A. Karthikeyan, C. Parthasarathy, B. B. Bright, Heat transfer analysis of latent heat storage system using d-sorbitol as pcm, ARPN Journal of Engineering and Applied Sciences 10 (2015) 5017–5021.